Research Square

Preprints are preliminary reports that have not undergone peer review.
They should not be considered conclusive, used to inform clinical practice,
or referenced by the media as validated information.

Novel 1,3-Indanedione Analogues as Anti-Arthritic Agents Targeting Interleukin-6

Akey Krishna Swaroop
Shri Vile Parle Kelavani Mandal's College of Pharmacy
M Esakkimuthukumar
JSS College of Pharmacy, JSS Academy of Higher Education and Research
Sai Varshini Magham
JSS College of Pharmacy, JSS Academy of Higher Education and Research
T K Praveen
JSS College of Pharmacy, JSS Academy of Higher Education and Research
Saranya Dharmaraj
JSS College of Pharmacy, JSS Academy of Higher Education and Research
Krishnan Namboori
Amrita Vishwa Vidyapeetham
Jawahar N Dr
JSS College of Pharmacy, JSS Academy of Higher Education and Research
Jubie Selvaraj
jubie@jssuni.edu.in

JSS College of Pharmacy, JSS Academy of Higher Education and Research

Research Article

Keywords: Interleukin-6, 1,3-indanedione, rheumatoid arthritis, computational screening, STAT-3, inflammatory disorders

Posted Date: August 31st, 2026

DOI: https://doi.org/10.21203/rs.3.rs-10712619/v1

License: This work is licensed under a Creative Commons Attribution 4.0 International License.
Read Full License

Additional Declarations: No competing interests reported.

Novel 1,3-Indanedione Analogues as Anti-Arthritic Agents Targeting Interleukin-6

Akey Krishna Swaroop[1], Esakkimuthukumar M[2], Sai Varshini Magham[3], Praveen T K[3], Saranya Dharmaraj[2], Krishnan Namboori P K[4], Jawahar N[5], Jubie Selvaraj[2*]

[1]Department of Pharmaceutical Chemistry, Shri Vile Parle Kelavani Mandal's College of Pharmacy, Shirpur, Maharashtra, India

[2]Department of Pharmaceutical Chemistry, JSS College of Pharmacy, JSS Academy of Higher Education and Research, Ooty, Tamilnadu, India

[3]Department of Pharmacology, JSS College of Pharmacy, JSS Academy of Higher Education and Research, Ooty, Tamilnadu, India

[4]Amrita Molecular Modeling and Synthesis (AMMAS) Research Lab, Amrita Vishwavidyapeetham, Amrita Nagar, Ettimadai, Coimbatore, Tamilnadu, India

[5]Department of Pharmaceutics, JSS College of Pharmacy, JSS Academy of Higher Education and Research, Ooty, Tamilnadu, India

Corresponding Author:

Dr. S. Jubie

Associate Professor

Department of Pharmaceutical Chemistry

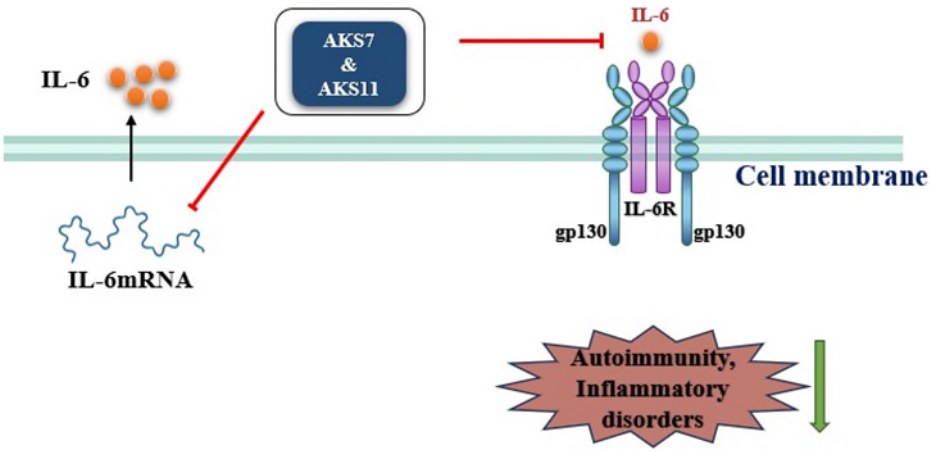
JSS College of Pharmacy

Udhagamandalam- 643001

Email: jubie@jssuni.edu.in

http://orcid.org/0000-0002-4633-6621.

Graphical Abstract:



Graphical abstract: *The designed molecules target IL-6 mRNA and IL-6 protein to disrupt its signaling network, aiming to reduce chronic inflammation.*

Abstract:

The interleukin-6(IL-6) signaling pathway plays a critical role in mediating inflammatory responses implicated in various diseases, including rheumatoid arthritis. The synthesis of new class of 1,3-indanedione AKS1-AKS12 was guided by their favorable binding affinities to the IL-6 receptor identified through in-silico approaches in wild and mutated-proteins. Characterization of synthesized compounds was performed using FTIR, NMR, and Mass spectroscopy. *In-vitro* assays, including MTT, RT-PCR, and ELISA, were conducted to assess the efficacy of AKS1-AKS12 in modulating IL-6 overexpression. Acute oral toxicity studies were conducted to evaluate the safety profiles of the compounds, while a rat model of Complete Freund's adjuvant (CFA) arthritis was employed to assess their therapeutic efficacy. Among the synthesized compounds, AKS7 and AKS11 demonstrated potent inhibition of IL-6 overexpression, supported by *in-vitro* experimental validation. Furthermore, acute oral toxicity studies revealed favorable safety profiles of the compounds, and in-vivo studies in a rat model of CFA arthritis demonstrated significant mitigation of arthritis symptoms. Downregulation of key inflammatory genes IL-6 and STAT-3 further supported the candidacy of AKS7 and AKS11 as IL-6 inhibitors. Our synthesized compounds, particularly AKS7 and AKS11, exhibit dual modulatory actions on the IL-6 signaling pathway, effectively inhibiting IL-6-mediated inflammation at both the protein and mRNA levels. Additionally, the compounds also downregulated the STAT-3 gene which is overexpressed during the IL6 activation in IL-6/STAT-3 pathway. These findings underscore the therapeutic potential of our designed compounds for conditions associated with dysregulated IL-6/STAT-3 signaling pathways, AKS7 and AKS11 as promising candidates for the treatment of IL-6-mediated inflammatory disorders.

Keywords: Interleukin-6, 1,3-indanedione, rheumatoid arthritis, computational screening, STAT-3,inflammatory disorders.

1. Introduction

Cytokines are crucial signaling molecules that regulate various aspects of human biology beyond immune responses. From embryonic development to aging, they help maintain physiological balance. Interleukins, a subset of cytokines, play a significant role in immune communication and disorders. Understanding cytokine signaling is vital for grasping human health and disease (Dinarello 2007; Jones and Jenkins 2018; Swaroop et al. 2024). Interleukin-6 (IL-6) is a key proinflammatory cytokine that significantly impacts immune system dynamics. Dysregulation of IL-6 is linked to chronic inflammatory conditions and autoimmune disorders. IL-6, along with IL-11, IL-27, IL-31, and oncostatin M (OSM), contributes to chronic inflammation, autoimmunity, infectious diseases, and cancer, often serving as diagnostic or prognostic markers (Feldmann and Brennan 1996; Narazaki and Kishimoto 2022; Swaroop et al. 2022a). IL-6 was first identified in the 1970s by Dr. Tadamitsu Kishimoto and his group has been a leading figure at the Laboratory of Immune Regulation in the Department of Medicine at Osaka University in Japan. His pioneering work there has greatly contributed to the field of immunology, particularly regarding the IL-6 cytokine and its effects on inflammation and autoimmunity. Key milestones in its research include the cloning of IL-6 cDNA and the development of anti-IL-6R antibodies and IL-6 knockout mice. The discovery of 'trans-signaling' and therapeutic agents like Tocilizumab and sgp130Fc marked significant advancements. Recent research has explored IL-6's applications in treating sepsis, enhancing bone healing, and addressing conditions like rheumatoid arthritis and COVID-19 (Tanaka and Kishimoto 2014; Kang et al. 2015; Choy et al. 2020; Kishimoto and Kang 2022). IL-6 influences cellular responses through three signaling modes: classic signaling, trans-signaling, and trans-presentation. Classic signaling involves IL-6 binding to membrane-bound IL-6R and gp130, aiding antibacterial activities. Trans-signaling, triggered by the cleavage of IL-6R to form sIL-6R, promotes rapid proinflammatory responses (Rose-John 2018). Trans-

presentation, seen in dendritic cell-T cell interactions, activates pathogenic Th17 responses. These modes collectively regulate diverse biological activities, underscoring IL-6's critical role in immune homeostasis and responses to physiological and pathological conditions (May et al. 2009; Tanaka et al. 2012; Garbers et al. 2012; Schaper and Rose-John 2015). The signaling mechanisms of IL-6 involve three main pathways downstream of gp130. The first pathway activates Janus kinase (JAK) and signal transducer and activator of transcription 3 (STAT3), leading to gene regulation (Heinrich et al. 2003; Jones et al. 2010). The second pathway involves the JAK and SHP-MAPK cascade, activating NF-κB through the PI3K-Akt pathway. The third pathway enhances YAP-NOTCH signaling via the Src kinase family member Yes, crucial in carcinogenesis. These cascades play vital roles in various diseases, with negative feedback regulation by STAT3 and suppressor of cytokine signaling (SOCS) proteins (Skiniotis et al. 2005; Lesina et al. 2011; Mauer et al. 2014; Sommer et al. 2014). Overall, IL-6 signaling orchestrates cellular processes like proliferation, survival, differentiation, migration, immune regulation, and responses to oxidative stress (Tanaka and Kishimoto 2014; Hunter and Jones 2015).

1.1.Research Gap & Motivation

This study addresses the urgent need to mitigate the harmful effects of Interleukin-6 (IL-6) dysregulation, a major factor in chronic inflammation and autoimmune disorders. While IL-6 plays a crucial role in immune response and acute-phase reactions, its overexpression leads to serious health issues, including elevated inflammatory markers and disruptions in bone metabolism and albumin levels. Current treatments mainly use monoclonal antibodies (Notable anti-IL-6 monoclonal antibodies include tocilizumab, sarilumab, siltuximab, olokizumab, and clazakizumab. These antibodies are employed in the treatment of various inflammatory and autoimmune diseases by inhibiting IL-6 signaling.) (Cobleigh et al. 1999; Genovese et al. 2015; Salama et al. 2021), which also have drawbacks such as high cost, immunogenicity, and the

limited availability of small-molecule inhibitors. Our research aims to fill this gap by identifying novel small-molecule inhibitors targeting both wild and mutated forms of IL-6. This innovative approach offers a promising alternative to existing treatments and has the potential to significantly improve patient outcomes. By developing small bioactive molecules, we seek to overcome the limitations of monoclonal antibodies and provide more accessible and effective treatment options for IL-6-related diseases (Aqel et al. 2019; Kaur et al. 2020). The motivation for our work arises from the critical need to address the unmet medical needs in IL-6-related diseases. By advancing research and drug development, our study aims to make a meaningful impact on global health and enhance the quality of life for millions worldwide. Currently, there are no small molecules approved for IL-6 inhibition primarily due to challenges in achieving high specificity, as small molecules often interact with multiple targets, leading to off-target effects. Additionally, designing small molecules that effectively block protein-protein interactions, such as those involving IL-6 and its receptor, is technically challenging. Mutations in IL-6 can further complicate small molecule binding. However, our in-silico studies have successfully identified promising docking scores for both wild-type and mutated IL-6 proteins, highlighting the potential of our designed molecules. This research paves the way for more effective small molecule therapies targeting IL-6, potentially bringing them to market. Ultimately, our goal is to discover new IL-6 inhibitors, paving the way for improved patient care and better management of IL-6-related disorders (Hirose et al. 2002; Hong et al. 2015).

1.2.Hypothesis

We hypothesize that targeting both IL-6 mRNA and IL-6 protein production during inflammatory conditions with our designed molecules will disrupt the intricate IL-6 signaling network, thus mitigating chronic inflammation. Inflammation begins with triggers like lipopolysaccharides (LPS), which activate toll-like receptors (TLRs). TLRs initiate a complex signaling cascade that leads to the activation of nuclear factor kappa B (NF-κB), a key

transcription factor regulating inflammatory gene expression. One of these genes is IL-6, a potent pro-inflammatory cytokine. Once IL-6 mRNA is transcribed, it is stabilized in the nucleus by ARID5, then exported to the cytoplasm for translation into IL-6 protein. The secreted IL-6 binds to its receptor, activating the gp130 receptor subunit and triggering intracellular signaling pathways such as Janus kinase/signal transducer and activator of transcription 3 (JAK/STAT3), Ras/mitogen-activated protein kinase (MAPK), and phosphoinositide 3-kinase/protein kinase B (PI3K–PKB/AKT). These pathways amplify the inflammatory response, perpetuating chronic inflammation (Schaper and Rose-John 2015; Copaescu et al. 2020; Nyati and Kishimoto 2022, 2023). We specifically aim to check whether our designed compounds downregulate STAT-3, a key downstream signaling gene overexpressed during IL-6 activation in the IL-6/STAT-3 pathway. We believe that our molecules can effectively interfere with this pathway, demonstrating their therapeutic potential for conditions associated with dysregulated IL-6/STAT-3 signaling pathways which is shown in **Figure 1.**

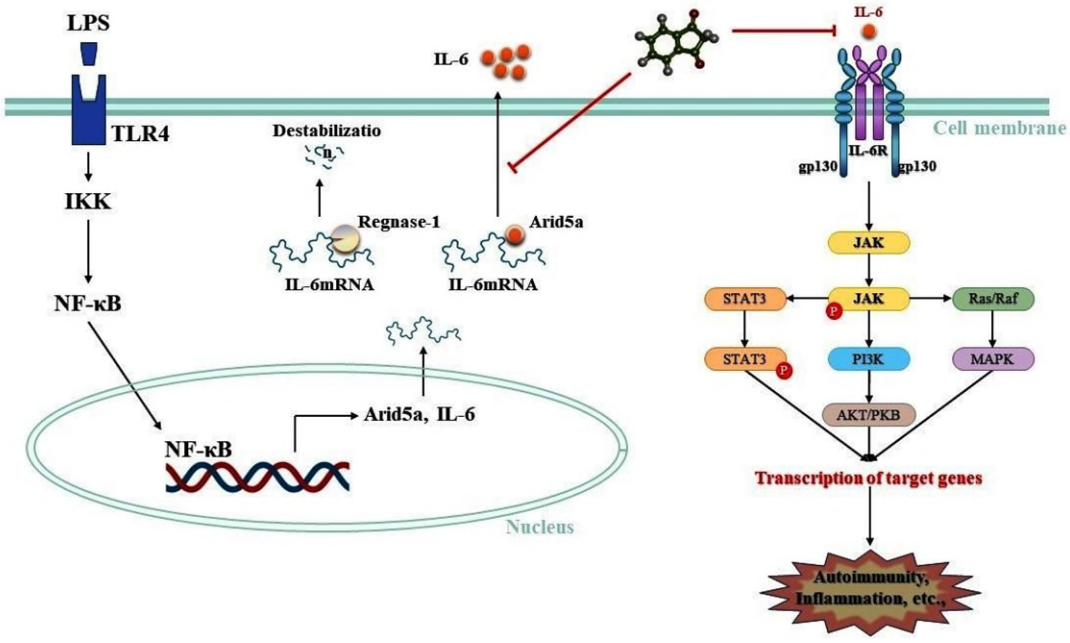


Figure 1. *Hypothesis (Modulation of IL-6 mediated signalling pathways by novel small bioactive molecules)*

1.3.Rationale for Selecting Indane-1,3-dione

The selection of indane-1,3-dione as a potential inhibitor of Interleukin-6 (IL-6) is based on a thorough review of literature and medicinal chemistry principles (Mitka et al. 2009; Pluskota and Koba 2018). Previous studies have shown the efficacy of indole-based compounds in inhibiting IL-6, which led us to explore a novel approach (Tagat et al. 1995; Li et al. 2013; Furman et al. 2014; Aqel et al. 2019) . By substituting the nitrogen atom in indole with a methylene group (CH_2), we created a unique medicinal chemistry library featuring an indane moiety, offering a new perspective in IL-6 inhibition. Historically, cyclic diketone derivatives of indane-1,3-dione have been used in various applications, such as anti-coagulants, insecticides, and rodenticides (Asadi and Mohammadi Ziarani 2016). These compounds have demonstrated diverse bioactivities, including antiviral, anti-inflammatory, antifungal, antibacterial, antiparasitic, and antiproliferative properties (Meena et al. 2006; Verma et al. 2014). Indane-1,3-dione hydrazine derivatives with benzimidazole moiety having human neutrophil elastase inhibition (S. et al.). This wide range of bioactivities highlights the potential of indane-1,3-dione derivatives in therapeutic interventions for IL-6-related disorders. The distinctive 1,3-dicarbonyl structure of indane-1,3-dione derivatives gives them specific physicochemical properties suitable for organic chemistry studies. The presence of two carbonyl groups separated by a single carbon atom influences their reactivity patterns and pharmacological responses. This structural feature, along with the enolization effect, contributes to their varied pharmacological activities. In conclusion, the rationale for selecting indane-1,3-dione for IL-6 inhibition is based on its historical use, diverse bioactivities, distinctive physicochemical properties, and broader synthetic applications (Frédérick et al. 2006; Singh 2016). This rationale underscores the potential of this class of compounds as novel inhibitors of IL-6, offering new therapeutic avenues for IL-6-related disorders.

2. Methods and Materials

2.1.*In silico* computational studies:

Our research aims to address a critical gap in current drug development efforts by identifying novel small molecules for IL-6 inhibition. While numerous small bioactive molecules have shown promise in *in vitro* and *in vivo* studies, none have progressed to commercialization. One major contributing factor to this lack of success may be the presence of mutations in the IL-6 protein, which can affect the binding of small molecules and reduce their potency, as observed in the context of COVID-19 and other diseases (Akey et al. 2021). To address this, we conducted comprehensive *in silico* computational studies encompassing pharmacogenomics, proteomics, molecular docking, ADMET studies, and molecular dynamics simulations (Swaroop et al. 2022b; B. S. et al. 2023; Krishna Swaroop et al. 2023). First, we utilized pharmacogenomics analysis to identify mutations at the binding sites of IL-6. Subsequently, proteomics studies were employed to map these mutations in the wild-type protein. Molecular docking studies were then conducted for both the wild-type and mutated proteins to assess the binding affinity of our novel designed molecules. This allowed us to determine if our molecules could effectively bind to both wild-type and mutated IL-6 proteins. Furthermore, ADMET studies using Data Warrior were employed to evaluate the safety and efficacy of our IL-6 inhibitors. This step was crucial in ensuring that our designed molecules met the necessary criteria for further development. Lastly, molecular dynamics simulations using the Schrödinger Suite Desmond module were conducted to assess the stability of the protein-drug complexes for both wild-type and mutated proteins (Namboori 2021; M et al. 2022; Krishna Swaroop et al. 2022; Mude et al. 2023; Patnaik et al. 2024). By employing these comprehensive *in silico* computational studies, we gained valuable insights into the potential of our designed molecules to effectively inhibit IL-6 activity, both in its wild-type and mutated forms. These findings lay the groundwork for further experimental validation and the development of novel therapeutics for IL-6-related diseases.

2.2.Synthesis of 1,3 indane dione derivates:

We synthesized twelve compounds following a standard protocol for reproducibility and ease of synthesis:

Step 1: C-Alkylation of 1,3-Indanedione

1,3-Indanedione (5g, 0.03 mol), ethyl chloroacetate (6.4 ml, 0.06 mol), and potassium carbonate (2.7g, 0.02 mol) were refluxed in chloroform at 60°C for 8 h. A dark brown precipitate formed, which was filtered, dried, and recrystallized using chloroform to yield ethyl 2-(1,3-dioxo-2H-inden-2-yl) acetate (Meena et al. 2006; D. et al. 2007; Mitka et al. 2009).

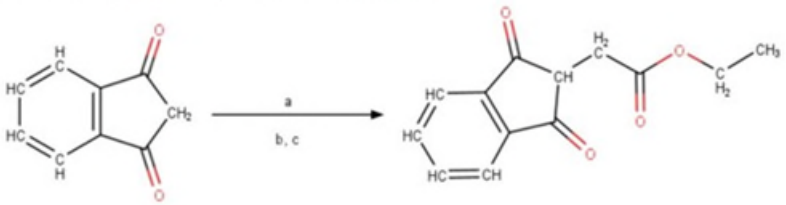
Step 2: Formation of Hydrazones

Aromatic aldehydes or acetophenones (0.025 mol) were dissolved in ethanol (30 ml) and reacted with hydrazine hydrate (0.05 mol, 1.6 ml) at 60°C for 4 h. The reaction mixture was poured into crushed ice, yielding a solid precipitate, which was dried and recrystallized using ethanol (Verma et al. 2014).

Step 3: Synthesis of 1,3-Indanedione Hydrazone Derivatives

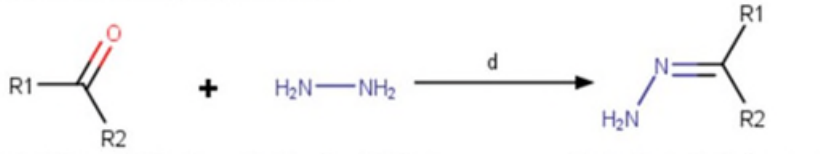
Ethyl 2-(1,3-dioxo-2H-inden-2-yl) acetate (1 mol) was reacted with hydrazones (1.5 mol) in chloroform at 60°C for 12 h. The resulting solid precipitate was filtered, dried, and recrystallized using chloroform to obtain the final compounds. The synthesized compounds are detailed in Table 2.

Step 1: *C-Alkylation of 1,3-Indanedione*



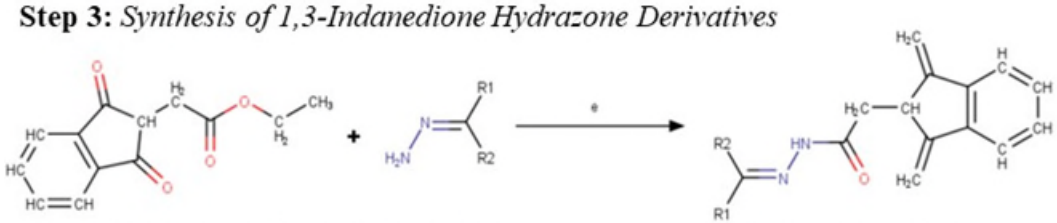
1,3-indandione Ethyl 2-(1,3-dioxo-2H-inden-2-yl)acetate

Step 2: *Formation of Hydrazones*



Substituted Benzaldehydes / Acetophenones Hydrazine Hydrate Substituted Hydrazone

Step 3: *Synthesis of 1,3-Indanedione Hydrazone Derivatives*



Ethyl 2-(1,3-dioxo-2H-inden-2-yl)acetate Substituted Hydrazone 1,3-indandione Hydrazone derivatives

Reagents and conditions

a) Ethyl chloroacetate (ClCH2COOEt),

b) Potassium carbonate (K2CO3),

c) Chloroform (CHCl3), Reflux 8 h with continuous stirring at 60°C, 300 rpm.

d) Ethanol (C2H5OH), reflux 4 h with continuous stirring at 60°C, 300rpm.

e) Chloroform (CHCl3), reflux 12 h with continuous stirring at 60°C, 300 rpm.

2.3.*In-vitro* evaluation for synthesized compounds:

2.3.1. MTT Assay for Cytotoxic Effect:

The cytotoxic effects of the synthesized compounds were evaluated using the RAW264.7 cell line, maintained in DMEM with 10% FBS and necessary supplements. Cells were seeded in 96-well plates at $5x10^3$ cells per well and incubated at 37°C with 5% CO2. Compounds were

prepared by dissolving 1mg in 1mL of 0.1% DMSO, filtered for sterility, and serially diluted to concentrations ranging from 100µg to 6.25µg. After 24 h of incubation, the medium was replaced with compound solutions in triplicate, with untreated cells as controls. Post-treatment, cells were examined microscopically for morphological changes indicative of cytotoxicity. For the MTT assay, 15 mg MTT in PBS was added to each well and incubated for 4 h to form formazan crystals, which were then dissolved in DMSO. Absorbance was measured at 540 nm to calculate growth inhibition percentages (Begam et al. 2019; Chenicheri et al. 2022; Selvaraj et al. 2023).

The percentage of growth inhibition was calculated using the form

% of viability = Mean OD of sample / Mean OD of control group x 100%

2.3.2. Indirect ELISA

After attaining sufficient confluency, cells were induced with LPS(1µg/ml) for one hour, 25µg/ml of each sample was added and incubated for 24 h Non-treated control and LPS-induced wells were also maintained and incubated for 24 h (Elangovan et al. 2022). After incubation, the supernatant was collected and 100µL of each was added to the 96 well plates and kept in incubation for 37^0 c overnight. The following day, the wells were drained and washed with PBS 2 times. 200µl of freshly prepared blocking buffer (0.2% gelatin in 0.05% Tween 20: Merck; Germany) in PBS was added and incubated for 1 h at room temperature. It was washed twice with PBS TWEEN. 100µl of the primary antibody was added and left for 2 h at room temperature. After incubation, it was washed with PBS TWEEN (2 times). 100µL of secondary antibody (HRP Conjugate, Santacruez, USA) was added and left for 1 h at room temperature. It was then washed with PBS TWEEN two times. 200µL of O- dianizdine hydrochloride (1mg/100ml methanol + 21ml citrate buffer pH 5 + 60ml H_2O_2: Sigma Aldrich, USA) was added and left for 30 minutes at room temperature. The reaction stopped by adding

5N HCL (50µl). OD was read at 415 nm in an ELISA reader. The concentration of protein was also estimated (Wang et al. 2020; Peng et al. 2022).

Calculation

$$\textbf{\textit{The activity of Antibody}} = \frac{\textbf{\textit{OD value}}}{\textbf{\textit{Protein concentration}}}$$

2.3.3. Effect of synthesized drugs on IL-6 mRNA expression in RAW264.7 cells byReal-time PCR analysis

RAW264.7 cells were activated with LPS for one hour, followed by treatment with AKS7 and AKS11 samples at 25µg/ml concentration for 24 h at 37ºC in a humidified 5% CO2 incubator. Concurrently, LPS-stimulated control wells were processed for RNA isolation using the TRIzol method, followed by cDNA synthesis to assess relative IL-6 gene expression. All reactions were conducted in triplicate, and data analysis utilized the ΔΔCt method with Light Cycler 96 SW 1.1 Software. Primer sequences and melting temperatures (Tm) for GAPDH and IL-6 genes were utilized for Ct value determination.

2.3.3.1. Calculation of ΔCt values

By using the average Ct values, we computed the ΔCt value of LPS, AKS7, AKS11 treated, and untreated control. Below is the formula for calculating ΔCt value.

$$\Delta Ct = Ct\ (IL-6) - Ct(GAPDH)$$

2.3.3.2. Calculation of ΔΔCt values

The ΔΔCt values of each samples were then computed. The formula used for calculating ΔΔCt values as follows:

$$\Delta\Delta Ct = \Delta Ct\ (Sample) - Ct(Control)$$

2.3.3.3. Fold gene expression values

Finally, the fold gene expression values of each samples were calculated using two to the power of negative ΔΔCt to figure out the fold gene expression. The relevant formula for computing fold gene expression value is provided below.

$$Fold\ gene\ expression = 2\text{^} - (\Delta\Delta\mathrm{Ct})$$

Additionally, agarose gel electrophoresis was employed to visualize and analyze DNA fragments. A 1.5% agarose gel was prepared in 1x TE buffer with ethidium bromide, and electrophoresis at 50 V for 30 minutes separated the samples. Gel analysis and documentation were performed using a gel documentation system for further validation and visualization of results (Cai et al. 2020; Selvaraj et al. 2023).

2.4.*In-vivo* animal studies

2.4.1. Acute toxicity study

In our *in-vivo* animal studies, we conducted an acute oral toxicity assessment of compounds AKS7 and AKS11 following OECD-423 guidelines in female Swiss albino mice. Each compound was administered orally at a single dose of 2000 mg/kg, and the mice were observed over a 14-day period for any immediate or delayed adverse effects. Ethical approval (IAEC approval number: JSSCP/OT/IAEC/22/2022-2023) ensured adherence to humane treatment standards throughout the study.

2.4.2. Complete Freund's adjuvant-induced arthritis

For the evaluation of anti-arthritic activity, animals were categorized into seven distinct groups. The Normal Control (Group I) received no treatment, while the Arthritic Control (Group II) was induced with Complete Freund's adjuvant (CFA) to simulate arthritis. Methotrexate (Group III) served as a positive control, administered subcutaneously at 3 mg/kg twice weekly. Groups IV and V were orally administered AKS7 at low (50 mg/kg) and high (100 mg/kg) doses, respectively, while Groups VI and VII received AKS11 at the same low and high doses. This experimental setup facilitated the assessment of AKS7 and AKS11's potential as anti-arthritic agents under controlled conditions (Ingawale and Patel 2018; Chen et al. 2020).

2.4.3. Anti-arthritic activity

Throughout the 28-day treatment period, efficacy was monitored using weekly measurements of paw volume and arthritic scores, evaluated via visual scoring on a 5-point scale. Body weights were also recorded weekly to monitor overall animal health and treatment tolerance. On Day 28, blood samples were collected to assess IL-6 levels through ELISA and RT-PCR analyses, providing insights into the compounds' modulation of inflammation. Following euthanasia, ankle joints were histopathological examined to evaluate treatment effects at a tissue level. Additionally, Real-time PCR analysis was conducted on tissue samples to investigate the impact of AKS7 and AKS11 on IL-6 mRNA and STAT-3 mRNA expression levels (Kamel et al. 2018). Standard protocols for RNA extraction, qRT-PCR, and gel electrophoresis were followed to ensure the specificity and reliability of the results. These molecular analyses aimed to elucidate the underlying mechanisms by which AKS7 and AKS11 exert their anti-arthritic effects, providing crucial data for their potential therapeutic applications in arthritis management. Primer sequences used for IL-6, STAT3, and GAPDH genes are summarized in **Table 1.** These analyses provided valuable data on the molecular mechanisms underlying the therapeutic effects of the compounds in arthritis.

Table 1. *Primer sequences used for IL-6, STAT3, and GAPDH genes*

S.NO.	**OLIG O NAME**	**FORWARD**		**REVERSE**	
		SEQUENCE (5' ->3')	Tm	SEQUENCE (5' ->3')	Tm
1	**IL-6**	GGTACATCCTCGACGG CATC T	61.8	GTGCCTCTTTGCTGCTTTC AC	59.8
2	**STAT 3**	GCGAGTTCCCCATGGA	54.3	CACGAGTGTGACT	40
3	**GAPD H**	AATGCATCCTGCACCAC CAA CTGC	64.4	GGAGGCCATGTAGGCCAT GA GGTC	67.8

3. Results and discussion

3.1. *In-silico* results

3.1.1. Pharmacogenomics of Ensembl Variant Effect Predictor (VEP) & Mapping of proteins sequences by collected mutations

Our *in-silico* investigation commenced with pharmacogenomics studies, wherein we initially amassed 3600 Single Nucleotide Polymorphisms (SNPs) associated with IL-6 from the NCBI database. These SNPs were subsequently inputted into the Ensembl Variant Effect Predictor (VEP) database for analysis. VEP scrutinizes the effect of IL-6 variants on genes, transcripts, protein sequence, and regulatory regions. Among the 34,633 samples analyzed, based on our summary statistics, we collected genetic variations and their predicted effects using VEP, approximately 66% exhibited missense variants altering protein function. Notably, the IL-6 protein (PDB ID: 1ALU) was identified with a genomic location at 7p15.3 (Chromosome 7, NC_000007.14). The determination of binding sites on the protein revealedcritical amino acid residues, including *40Arg (40R), 51Glu (51E), 75Gln (75Q), 76Ser (76S), 156Gln (156Q), 164His (164H), 168Arg (168R), 175Gln (175Q), 179Arg (179R), 182Arg (182R), and 183Gln (183Q)*. Subsequently, 12 mutations associated with these binding sites were identified from the Ensembl database. The variants, namely rs1021620720,rs190436077, rs1583433435, rs747126003, rs202210223, rs376403172, rs769825619, rs143432552, rs1488521608, and rs1326968679, were found to be present within the bindingsites of the 1ALU protein structure. The **Table 2.** presents the identification of 12 mutations associated with the binding sites from the Ensembl database. Each mutation is characterizedby its respective variation (rs ID), protein position, amino acid change, codon change, allele, and consequence. Here's a summary of the mutations: These mutations introduce amino acid substitutions at specific positions within the IL-6 protein sequence, potentially influencing

its structure and function. The consequences of these missense variants underscore their potential impact on protein function, highlighting their relevance to our investigation into IL-6 inhibition. Given the focus of our study on elucidating the interactions between designed compounds and the 1ALU protein in the presence of mutations, we mapped these mutations onto the IL-6 protein structure using SwissPDB Viewer software. This step facilitated a comprehensive understanding of how the mutations might influence the binding affinity and efficacy of the designed compounds, guiding our subsequent experimental investigations.

Table 2. Identification of 12 mutations related to the binding sitesfrom the Ensembl database

S.NO.	Uploaded variation	Protein position	Amino acids	Codons	Allele	Consequence
1	rs1021620720	68 (40)	R/K	aGa/aAa	A	missense_variant
2	rs190436077	79 (51)	E/Q	Gaa/Caa	C	missense_variant
3	rs1583433435	103 (75)	Q/E	Caa/Gaa	G	missense_variant
4	rs747126003	103 (75)	Q/R	cAa/cGa	G	missense_variant
5	rs747126003	103 (75)	Q/L	cAa/cTa	T	missense_variant
6	rs202210223	104 (76)	S/Y	tCt/tAt	A	missense_variant
7	rs376403172	184 (156)	Q/E	Cag/Gag	G	missense_variant
8	rs769825619	196 (168)	R/C	Cgc/Tgc	T	missense_variant
9	rs143432552	196 (168)	R/H	cGc/cAc	A	missense_variant
10	rs143432552	196 (168)	R/L	cGc/cTc	T	missense_variant
11	rs1488521608	210 (182)	R/W	Cgg/Tgg	T	missense_variant
12	rs1326968679	210 (182)	R/Q	cGg/cAg	A	missense_variant

3.1.2. Proteomics

Following the identification and mapping of mutations onto the 1ALU protein structure, the

subsequent step in our *in-silico* analysis involved proteomics. Here, we validated the mutated protein structure by employing a Ramachandran plot, comparing it with the wild protein usingthe saves v6.0 webserver. The Ramachandran plots for both the wild and mutated proteins were analyzed according to the south Asian population. The wild protein's plot is depicted in **Figure 2a**, while the mutated protein's plot is shown in **Figure 2b**. From these plots, we observed that both the wild and mutated proteins exhibited a similar number of residues in favorable regions, with none in the disallowed regions. This suggests that the protein structure retains flexibility in certain regions, potentially allowing for slight conformational changes without compromising its overall structure and function. Such flexibility could contribute to the binding affinity observed for both wild and mutated proteins. These findings imply that both thewild-type and mutated proteins retain structural integrity and flexibility, which may facilitate their binding affinity with the designed 1,3 indanedione derivatives.

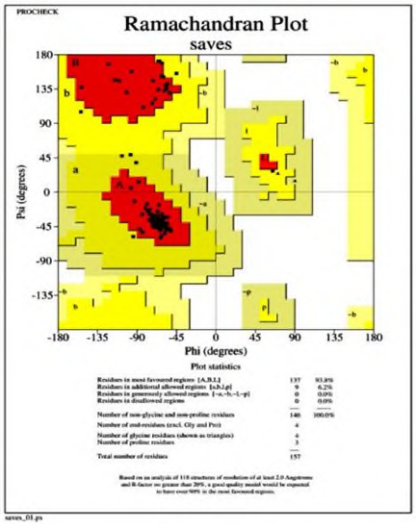


Figure 2a. *Ramachandran plotfor 1ALU wild protein*

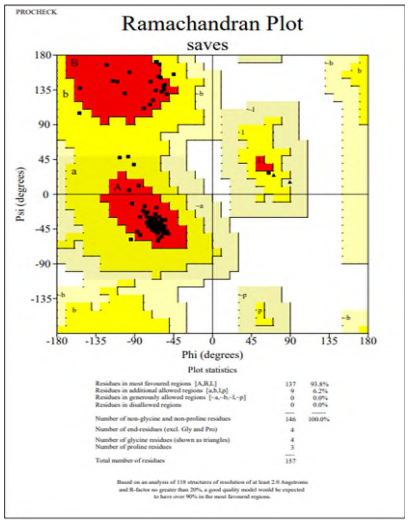


Figure 2b. *Ramachandran plotfor 1ALU mutated protein*

3.1.3. Molecular docking

In our molecular docking analysis, AKS11 and AKS7 exhibited strong binding affinities towards both wild-type and mutated IL-6 proteins, with affinities ranging from -8.1 to -8.4 kcal/mol and -8.1 to -8.3 kcal/mol, respectively. These results highlight their robust interactions with the IL-6 protein, suggesting their potential as effective modulators of IL-6 activity. In contrast, MDL A displayed weaker binding affinities, particularly towards mutated IL-6 proteins, with values decreasing from -6.2 kcal/mol for wild-type to -5.1 kcal/mol for mutated proteins. This difference indicates potential challenges for MDL A in effectively engaging with mutated forms of IL-6, potentially limiting its therapeutic efficacy in scenarios involving protein mutations. Overall, the strong binding affinities of AKS11 and AKS7 underscore their versatility and effectiveness as promising candidates for further pharmaceutical development aimed at modulating IL-6 activity which is shown in **Table 3.**

3.1.4. ADMET analysis

The ADMET (Absorption, Distribution, Metabolism, Excretion, and Toxicity) properties of the designed molecules were evaluated to assess their potential as drug candidates which showed in **Table 4.** Additionally, the ADMET analysis revealed favorable drug-like properties for the designed molecules, including optimal molecular weights, cLogP, cLogS values, and acceptable numbers of hydrogen bond acceptors/donors and polar surface area. These findings support their potential for absorption, distribution, metabolism, excretion, and minimal toxicity, enhancing their suitability as potential anti-inflammatory agents targeting IL-6.

3.1.5. MMGBSA *results for designed molecules against both wild and mutated proteins*

Furthermore, MMGBSA results reaffirmed the strong binding interactions of AKS11 and AKS7 with both wild-type and mutated IL-6 proteins, with significantly lower binding free energies compared to MDL A. AKS11 exhibited binding free energies ranging from -76.10 to -80.12 kcal/mol, while AKS7 displayed energies ranging from -74.71 to -79.82 kcal/mol. These results

further substantiate the robust binding capabilities of AKS11 and AKS7, supporting their potential as effective IL-6 modulators across different protein variants which is shown **Table 5.** In conclusion, AKS11 and AKS7 show promising potential as therapeutic agents for targeting IL-6 activity, supported by their strong binding affinities, favorable ADMET profiles, and low binding free energies in MMGBSA analysis. Future studies should focus on validating these findings through *in vitro* and *in vivo* experiments to fully explore their therapeutic efficacy and safety profiles in treating IL-6-related disorders.

Table 3. *Molecular docking results for designed molecules against both wild and mutated proteins*

Compounds	WIL D protein (kcal /mol)	Lys40 (kcal/ mol)	Gln51 (kcal/ mol)	75arg (kcal/ mol)	75glu (kcal/ mol)	75leu (kcal/ mol)	76tyr (kcal/ mol)	156gl u (kcal/ mol)	168cy s (kcal/ mol)	168hi s (kcal/ mol)	168le u (kcal/ mol)	182gl n (kcal/ mol)	182trp (kcal/ mol)	All mutati ons (kcal/ mol)
AKS11	-8.1	-8	-8	-7.9	-7.9	-8	-8.1	-8.1	-8.1	-8.2	-8.1	-8	-8.1	-8.4
AKS7	-8.1	-7.6	-7.7	-7.8	-7.8	-7.7	-7.7	-7.5	-7.1	-8.1	-7.8	-7.7	-7.8	-8.3
AKS6	-7.2	-7.4	-6.6	-7.4	-7.4	-7.4	-7.4	-6.4	-6.6	-7.4	-7.2	-7.4	-7.3	-7.3
AKS5	-7.1	-7.2	-6.7	-7.2	-7.2	-7.2	-6.3	-6.7	-6.9	-7.2	-7.2	-7.2	-7.2	-7.3
AKS9	-7	-6.7	-6.7	-6.6	-7.1	-6.6	-6.7	-7.1	-6.8	-7.1	-6.7	-6.6	-6.7	-7
AKS10	-6.9	-7	-7	-7	-7	-7	-7	-7	-6.6	-6.9	-7	-6.6	-7	-7
AKS8	-6.9	-7.1	-7.2	-7.1	-7.1	-7.1	-7.2	-6.9	-6.8	-7.1	-7.2	-7.1	-7.5	-7.4
AKS2	-6.8	-6.8	-7.4	-7	-7	-7	-6.9	-6.6	-6.6	-6.9	-7	-7	-7.4	-7.2
AKS1	-6.7	-6.8	-6.8	-6.8	-6.9	-6.8	-6.5	-6.7	-6.3	-6.6	-6.8	-6.8	-6.7	-7.1
AKS3	-6.6	-6.3	-6.8	-6.8	-6.8	-6.7	-6.7	-6.6	-6.1	-6.7	-6.8	-6.5	-6.8	-6.9

AKS4	-6.5	-6.9	-6.9	-6.9	-6.9	-6.9	-6.9	-6.8	-6.6	-7	-6.9	-6.9	-6.9	-6.9
AKS12	-6.3	-6.6	-6.7	-6.6	-6.6	-6.5	-6.5	-6.7	-6.5	-6.6	-6.5	-6.6	-6.7	-6.9
MDL A	-6.2	-5.6	-5.3	-5.5	-5.2	-5.5	-5.2	-5.6	-5.4	-5.5	-5.3	-5.5	-5.2	-5.1
METHOTREXATE	-7.2	-6.5	-6.4	-6.3	-6.5	-6.6	-6.6	-6.3	-6.2	-6.8	-6.4	-6.3	-6.4	-6.3
(Co-crystal)	-4.9	-5	-4.8	-4.8	-5	-4.8	-5	-5	-5.1	-5	-5	-4.6	-5	-5

Table 4. ADMET properties for designed molecules by using Data warrior software.

Molecule	Total Molweight	cLogP	cLogS	HBA	HBD	PSA	Mutagenic	Tumorigenic	Reproductive Effective	Irritant
AKS1	350.373	2.745	-5.175	6	1	84.83	none	none	none	None
AKS2	399.243	3.5402	-5.991	5	1	75.6	none	none	none	None
AKS3	327.363	1.6451	-5.187	6	1	116.73	none	none	none	None
AKS4	296.281	2.0658	-5.479	6	1	88.74	none	none	none	None
AKS5	307.308	1.9302	-5.026	6	1	88.49	none	none	none	None
AKS6	351.317	1.9555	-5.257	8	1	121.42	none	none	none	None

AKS7	351.317	1.9555	-5.257	8	1	121.42	none	none	none	None
AKS8	340.765	3.4831	-5.533	5	1	75.6	none	none	none	None
AKS9	322.319	2.5314	-5.501	6	2	95.83	none	none	none	None
AKS10	340.765	3.4831	-5.533	5	1	75.6	none	none	none	None
AKS11	356.38	4.0715	-5.403	5	1	75.6	none	none	none	None
AKS12	306.32	2.8771	-5.797	5	1	75.6	none	none	none	None
MDL A	311.42	3.6992	-3.354	5	1	66.84	none	none	none	None
Methotrexate	454.446	-1.2285	-3.767	13	5	210.54	none	high	none	None
Limits	<500	<5	>-5	<10	<5	<200	None	None	None	None

Table 5. *MMGBSA results for designed molecules against both wild and mutated proteins*

Compounds	WILD protein (kcal/mol)	Lys40 (kcal/mol)	Gln51 (kcal/mol)	75arg (kcal/mol)	75glu (kcal/mol)	75leu (kcal/mol)	76tyr (kcal/mol)	156glu (kcal/mol)	168cys (kcal/mol)	168his (kcal/mol)	168leu (kcal/mol)	182gln (kcal/mol)	182trp (kcal/mol)	All mutations (kcal/mol)
AKS11	-78.12	-76.41	-77.98	-78.19	-76.42	-74.81	-74.32	-77.11	-74.12	-78.21	-76.10	-79.81	-79.12	-80.12
AKS7	-76.12	-75.62	-74.71	-75.28	-75.78	-75.27	-76.17	-77.15	-76.11	-77.71	-76.81	-79.71	-79.82	-79.23
AKS6	-72.22	-72.24	-76.16	-71.14	-71.21	-71.97	-70.42	-69.48	-72.64	-71.42	-70.21	-72.41	-72.33	-74.33
AKS5	-70.11	-70.32	-69.70	-67.22	-67.55	-67.21	-66.43	-66.79	-68.99	-70.21	-69.20	-70.12	-70.21	-71.23
AKS9	-68.54	-67.27	-68.17	-65.56	-65.11	-65.62	-67.77	-67.11	-69.84	-69.71	-64.27	-69.36	-68.37	-70.11
AKS10	-65.19	-64.11	-62.11	-61.09	-61.11	-61.32	-61.21	-63.53	-63.66	-65.19	-61.27	-65.90	-65.12	-66.98
AKS8	-63.19	-62.11	-61.20	-60.32	-60.21	-59.32	-60.11	-61.90	-59.18	-62.32	-60.43	-62.23	-63.54	-64.32
AKS2	-61.80	-60.81	-60.34	-59.43	-58.42	-57.55	-57.98	-60.62	-59.16	-61.29	-58.56	-61.43	-62.14	-63.12
AKS1	-56.70	-56.54	-56.18	-53.79	-53.69	-52.43	-54.55	-54.17	-54.30	-56.40	-55.28	-56.80	-56.71	-57.10
AKS3	-52.06	-52.03	-51.08	-49.28	-48.18	-49.17	-52.07	-51.16	-53.11	-55.32	-53.80	-53.85	-54.38	-54.90

AKS4	-48.35	-47.19	-46.44	-46.39	-46.07	-48.19	-47.94	-46.28	-48.62	-49.54	-47.39	-49.89	-50.90	-51.65
AKS12	-42.30	-41.36	-46.07	-43.36	-43.54	-43.27	-44.51	-42.04	-43.50	-44.16	-42.35	-43.60	-43.27	-44.87
MDL A	-56.21	-50.60	-49.23	-45.5	-45.23	-45.67	-46.32	-48.52	-46.32	-47.50	-44.32	-45.50	-44.32	-44.31
(Co-crystal)	-38.03	-39.15	-36.43	-34.67	-34.69	-34.74	-34.31	-36.14	-37.58	-37.43	-37.87	-37.44	-36.97	-37.67

3.1.6. Molecular dynamics simulation

Molecular dynamics simulation was employed to investigate the stability and dynamic behavior of the AKS11-ligand complexes with both wild-type and mutated IL-6 proteins over a 100 ns period. The RMSD analysis indicated stable Cα atom fluctuations, with values ranging from 2.4-2.8 Å for the AKS11-Wild complex and 2.0-3.2 Å for the AKS11-Mutated complex. Medium fluctuation RMSD for ligand-protein fitting showed ranges of 4.5-12.5 Å and 6.0-9.0 Å, respectively, suggesting overall stability in both complexes throughout the simulation. Root Mean Square Fluctuation (RMSF) analysis revealed low amino acid fluctuations (0.5–2.5 Å for AKS11-Wild and 0.5–3.0 Å for AKS11-Mutated), indicating minimal local changes along the protein chain. Protein-ligand contact analysis identified key interactions: in the AKS11-Wild complex, hydrogen bonds with Gln75, Gln175, Arg30, Arg179, and Arg182, along with electrostatic interactions with *Glu69, Arg30, Arg179,* and *Arg182* were prominent. Notably, *Arg179 (179R)* and *Arg182 (182R)* exhibited consistent hydrogen bond interactions. Conversely, the AKS11-Mutated complex showed hydrogen bonds *Lys40 (40K), Asn61 (61N), Leu62 (62L), Leu64 (64L), and Trp157 (157W)* alongside hydrophobic interactions involving several residues which is shown **Figure 3(a-f)**. These results underscore the stability and favorable interactions of AKS11 with both wild-type and mutated IL-6 proteins, supporting its potential as a stable and effective therapeutic candidate for modulating IL-6 activity. These findings warrant further exploration through experimental validation to confirm their therapeutic efficacy and safety profiles.

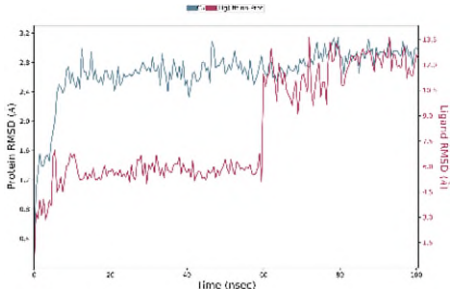


Figure 3a. *RMSD – AKS11 in wild protein.*

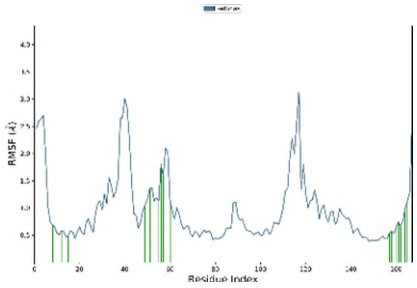


Figure 3b. RMSF – AKS11 in wild protein.

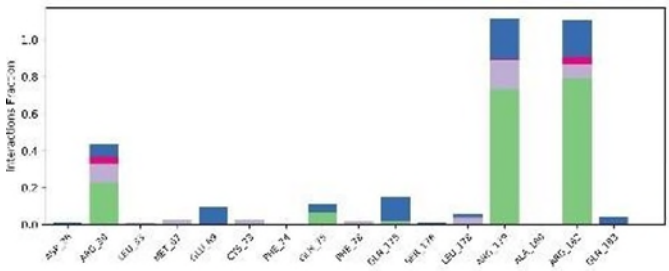


Figure 3c. *Protein ligand contacts – AKS11 in wild protein.*

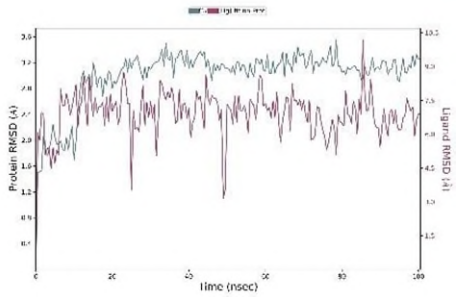


Figure 3d. *RMSD – AKS11 in mutated protein.*

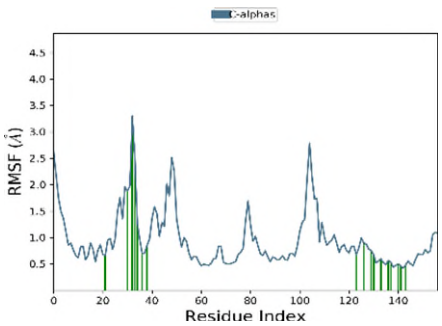


Figure 3e. *RMSF – AKS11 in mutated protein.*

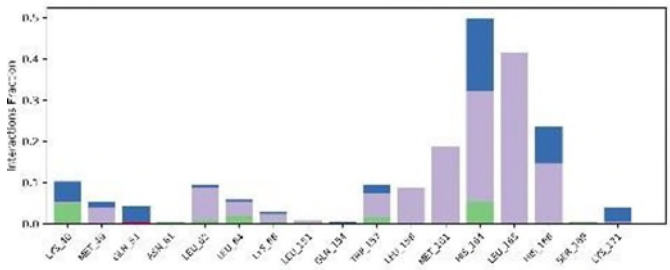


Figure 3f. *Protein ligand contacts – AKS11 in mutated protein*

3.2. Synthesis and characterization:

In the synthesis, the process begins with deprotonation where potassium carbonate (K_2CO_3) deprotonates the alpha-carbon of ethyl chloroacetate, forming an enolate intermediate, while chloroform ($CHCl_3$) acts as a solvent. The enolate then performs a nucleophilic attack on the electrophilic carbon of the CH_2 group in 1,3-indanedione, resulting in a beta-keto ester. Next, benzaldehyde/acetophenones reacts with hydrazine (N_2H_4) to form a Schiff base intermediate in the presence of ethanol (EtOH). Subsequently, the lone pair of electrons on the nitrogen atom of benzaldehyde/acetophenone hydrazine attacks the carbonyl carbon of ethyl 2-(1,3-dioxo-2H-inden-2-yl) acetate, forming a tetrahedral intermediate. This is followed by proton transfer from the hydrazine nitrogen to the ethoxy group, leading to the elimination of ethanol and the formation of a new amide bond. Finally, the elimination of the ethoxy group and subsequent bond rearrangement results in the formation of 2-(1,3-dioxo-2H-inden-2-yl)-N'-(E)-benzaldehyde/acetophenone methylidene] acetohydrazide as the amide product.

3.2.1. Characterizations of 2-(1,3-dioxo-2H-inden-2-yl)-N'-[(1Z)-1-(4-methoxyphenyl)ethylidene]acetohydrazide (AKS 1)

81% yield, Dark Brown colour, MP: 220-225^{o}C, Rf value: 0.52, FT-IR (cm^{-1}): 3480.23 (N-H str),3016.3 (CH_2 str), 2840.9 (C-H str), 1713.48 (C=O str), 1664.88 (NH-C=O str), 1593.67 (C=C str Ar), 1249.96 (C-O-C str). ^{1}H NMR (400MHZ, DMSO): δ ppm 8.8 (s, 1H, NH), 7.1(m, 4H, Ar-H), 7.9 (m, 4H, Ar-H), 6.6 (s, 1H, CH), 3.8 (d, 2H, CH_2), 1.2 (t, 1H, CH), 2.1 (s, 3H, CH_3). C^{13} NMR (400MHZ, DMSO): δppm 38.86 (CH_2), 40.12 (CH_3)55.44 (CH), 120- 135 (Ar

C), 144.73 (CH), 158.16 (C=O), 190, 195 (Ar C=O). Mass (m/z) – 350 ($C_{20}H_{18}N_2O_4$ M^+), 319 ($C_{19}H_{15}N_2O_3$ M^+), 203 ($C_{11}H_{13}N_2O_2$ M^{-2}), 143 ($C^9H^5O^2$ M^{-2}), 94 ($C_4H_6O_1N_2M^{-4}$), 84 ($C_2H_1N_2O_1$ M^{+1}), 71 ($C_2H_3N_2O_1$ M^{-1}).

3.2.2. Characterizations of N'-[(1Z)-1-(4-bromophenyl)ethylidene]-2-(1,3-dioxo-2H- inden-2-yl)acetohydrazide (AKS2)

86% yield, Light Brown colour, MP: 230-235°C, Rf value: 0.36, FT-IR (cm^{-1}): 3474.56 (N-Hstr), 2928.2 (CH_2 str), 2860.6 (C-H str), 1664.01 (C=O str), 1607.39 (NH-C=O str), 1569.19 (C=C str Ar), 760.68 (C-Br)

3.2.3. Characterizations of 2-(1,3-dioxo-2H-inden-2-yl)-N'-[(1Z)-1-(1,3-thiazol-2-yl)ethylidene]acetohydrazide (AKS3)

75% yield, Ash Brown colour, MP: 242-246°C, Rf value: 0.22, FT-IR (cm^{-1}): 3354.79 (N-H str),3066.23 (CH_2 str), 2856.8 (C-H str), 1642.26 (C=O str), 1605.70 (NH-C=O str), 1570.88 (C=Cstr Ar), 928 (C-S str). ^{1}H NMR (400MHZ, DMSO): δ ppm 8.9 (s, 1H, NH), 7.9 (m, 4H, Ar-H), 7.5 (m, 2H, Ar-H), 2.7 (s, 3H, CH_3), 2.2 (d, 2H, CH_2), 1.1 (t, 1H, CH). ^{13}CNMR (400MHZ, DMSO): δppm 16.40 (CH_3), 39.28 (CH_2) 54.20 (CH), 120-135 (Ar C), 140.32 (CH), 158.16 (C=O), 190, 195 (Ar C=O). Mass (m/z) - 327 ($C_{16}H_{13}N_3O_3S_1$ M+), 98 ($C_4H_6N_2O_1$ M^+), 84 ($C_3H_2N_1S_1$ M^+), 69 ($C_2H_3O_1N_2$ M^{-2}), 61 ($C_2H_3N_1O_1$ M^{-4}).

3.2.4. Characterizations of 2-(1,3-dioxo-2H-inden-2-yl)-N'-[(Z)-furan-2-ylmethylidene]acetohydrazide (AKS4)

68% yield, brownish black colour, MP: 215-220°C, Rf value: 0.42, FT-IR (cm^{-1}): 3408.54 (N-Hstr), 2920.6 (CH_2 str), 2849.3 (C-H str), 1640.15 (C=O str), 1613.93 (NH-C=O str), 1567.31 (C=C str Ar), 1292.99 (C-O-C str). ^{1}H NMR (400MHZ, DMSO): δ ppm 8.4 (s, 1H, NH), 7.3 (m, 4H, Ar-H), 7.1 (m, 3H, Ar-H), 6.6 (s, 1H, CH), 2.5 (d, 2H, CH_2), 1.1 (t, 1H, CH). ^{13}C NMR (400MHZ, DMSO): δppm 38.87 (CH_2), 50.12 (CH), 120-135 (Ar C), 150.48 (CH), 158.08 (C=O), 190, 195 (Ar C=O). Mass (m/z) – 296 ($C_{16}H_{12}N_2O_4$ M^+),142 ($C_9H_5O_2$ M^-

^{3}), 96 ($C_5H_4N_1O_1$ M^{+2}), 86 ($C_3H_4N_2O_1$ M^{+2}), 71 ($C_2H_3O_1N_2$ M^{-1}).

3.2.5. Characterizations of 2-(1,3-dioxo-2H-inden-2-yl)-N'-[(Z)-pyridin-2-ylmethylidene]acetohydrazide (AKS5)

65% yield, Tan brown colour, MP: 255-255ºC, Rf value: 0.64, FT-IR (cm^{-1}): 3407.69 (N-H str),2977 (CH_2 str), 2924.4 (C-H str), 1613.38 (C=O str), 1564.47 (NH-C=O str), 1493.58 (C=C strAr). ^{1}H NMR (400MHZ, DMSO): δ ppm 8.9 (s, 1H, NH), 7.4 (m, 4H, Ar-H), 7.2 (m,4H, Ar-H), 6.0 (s, 1H, CH), 2.9 (d, 2H, CH_2), 1.1 (t, 1H, CH). ^{13}C NMR (400MHZ, DMSO): δppm 39.49 (CH_2), 60.72 (CH), 120-135 (Ar C), 149.99 (CH), 169.26 (C=O), 188, 195 (Ar C=O). Mass (m/z) – 307 ($C_{15}H_{13}N_3O_3$ M^{+}), 164 ($C_8H_8N_3O_1$ M+2), 119 ($C_6H_6N_3$ M-1), 91 ($C_6H_5N_1$ M+), 82 ($C_3H_4N_2O_1$ M-2).

3.2.6. Characterizations of 2-(1,3-dioxo-2H-inden-2-yl)-N'-[(Z)-(2-nitrophenyl)methylidene]acetohydrazide (AKS6)

80% yield, Yellowish brown colour, MP: 247-252ºC, Rf value: 0.40, FT-IR (cm^{-1}): 3386.55 (N-H str), 2888.38 (CH_2 str), 2860.6 (C-H str), 1608.02 (C=O str), 1567.16 (NH-C=O str), 1520.18(C=C str Ar), 1406.53 (C-NO_2)

3.2.7. Characterizations of 2-(1,3-dioxo-2H-inden-2-yl)-N'-[(Z)-(3-nitrophenyl)methylidene]acetohydrazide (AKS7)

80% yield, Greyish brown colour, MP: 255-260ºC, Rf value: 0.28, FT-IR (cm^{-1}): 3386.69 (N-Hstr), 2920.6 (CH_2 str), 2860.6 (C-H str), 1628.20 (C=O str), 1570.56 (NH-C=O str), 1524.76 (C=C str Ar), 1347.11 (C-NO_2). ^{1}H NMR (400MHZ, DMSO): δ ppm 14.5 (s, 1H, NH), 7.7 (m, 4H, Ar-H), 7.4 (m, 4H, Ar-H), 6.8 (s, 1H, CH), 2.9 (d, 2H, CH_2), 1.2 (t, 1H, CH) ^{13}C NMR (400MHZ, DMSO): δppm 39.70 (CH_2), 59.55 (CH), 120-135 (Ar C), 148.31 (CH), 167.45 (C=O), 190, 195 (Ar C=O) Mass (m/z) - 351 ($C_{18}H_{13}N_3O_5$ M+), 204 ($C_9H_8N_3O_3$ M^{-2}), 144 ($C_9H_5O_2$ M^{-1}), 81 ($C_3H_4N_2O_1$ M^{-3}), 71 ($C_2H_3O_1N_2$ M^{+}).

3.2.8. Characterizations of N'-[(Z)-(4-chlorophenyl)methylidene]-2-(1,3-dioxo-2H-

inden-2-yl)acetohydrazide (AKS8)

82% yield, Greyish brown colour, MP: 222-228ºC, Rf value: 0.54, FT-IR (cm^{-1}): 3393.68 (N-Hstr), 2971.29 (CH_2 str), 2860.6 (C-H str), 1621.71 (C=O str), 1568.36 (NH-C=O str), 1525.64 (C=C str Ar), 732.62 (C-Cl)

3.2.9. Characterizations of 2-(1,3-dioxo-2H-inden-2-yl)-N'-[(Z)-(4-hydroxyphenyl)methylidene]acetohydrazide (AKS9)

84% yield, purple brown colour, MP: 240-245ºC, Rf value: 0.38, FT-IR (cm^{-1}): 3340.51 (N-H str), 2928.2 (CH_2 str), 2845.6 (C-H str), 1666.7 (C=O str), 1608.10 (NH-C=O str), 1569.66 (C=C str Ar), 2971.18 (OH str). ^{1}H NMR (400MHZ, DMSO): δ ppm 10.2 (s, 1H, NH),8.9 (s, 1H, OH), 7.0 (m, 4H, Ar-H), 7.4 (m, 4H, Ar-H), 6.7 (s, 1H, CH), 2.1 (d, 2H, CH_2), 1.2 (t,1H, CH). ^{13}C NMR (400MHZ, DMSO): δppm 38.86 (CH_2), 56.34 (CH), 120-135 (ArC), 144.73 (CH), 160.38 (C=O), 190, 195 (Ar C=O). Mass (m/z) - 322 ($C_{18}H_{14}N_2O_4M^+$), 148 ($C_9H_5O_2$ M^{+3}), 85 ($C_3H_4N_2O_1$ M^{+1}), 75 ($C_2H_3O_1N_2$ M^{+4}).

3.2.10. Characterizations of N'-[(Z)-(2-chlorophenyl)methylidene]-2-(1,3-dioxo-2H- inden-2-yl)acetohydrazide (AKS10)

79% yield, brownish black colour, MP: 237-242ºC, Rf value: 0.22, FT-IR (cm^{-1}): 3408.0 (N-H str), 2928.2 (CH_2 str), 2845.6 (C-H str), 1666.7 (C=O str), 1614.38 (NH-C=O str), 1569.77 (C=C str Ar), 750.83 (C-Cl). ^{1}H NMR (400MHZ, DMSO): δ ppm 9.0 (s, 1H, NH), 7.7(m, 4H, Ar-H), 7.4 (m, 4H, Ar-H), 6.6 (s, 1H, CH), 2.9 (d, 2H, CH_2), 1.2 (t, 1H, CH). ^{13}C NMR (400MHZ, DMSO): δppm 34.46 (CH_2), 60.56 (CH), 120-135 (Ar C), 144.75 (CH), 158.33 (C=O), 190, 195 (Ar C=O). Mass (m/z) - 340 ($C_{18}H_{13}Cl_1N_2O_3$ M^+), 304 ($C_{18}H_{13}N_2O_3$ M^{-1}), 184 ($C_8H_6Cl_1N_2O_1$ M^{+3}), 144 ($C_9H_5O_2$ M^{-1}), 88 ($C_3H_4N_2O_1$ M^{+4}), 74 ($C_2H_3O_1N_2M^{+3}$).

3.2.11. Characterizations of 2-(1,3-dioxo-2H-inden-2-yl)-N'-[(Z)-naphthalen-1-ylmethylidene] acetohydrazide (AKS11)

84% yield, Greyish brown colour, MP: 235-240ºC, Rf value: 0.42, FT-IR (cm^{-1}): 3443.55 (N-Hstr), 2971.24 (CH_2 str), 2841.8 (C-H str), 2323.71 (C=N str), 1670.5 (C=O str), 1608.97 (NH- C=O str), 1570.73 (C=C str Ar). ^{1}H NMR (400MHZ, DMSO): δ ppm 9.4 (s, 1H, NH),7.7 (m, 7H, Ar-H), 7.4 (m, 4H, Ar-H), 6.6 (s, 1H, CH), 2.9 (d, 2H, CH_2), 1.2 (t, 1H, CH). ^{13}C NMR (400MHZ, DMSO): δppm 32.46 (CH_2), 55.44 (CH), 120-135 (Ar C), 141.39 (CH), 167.32 (C=O), 190, 197 (Ar C=O). Mass (m/z) - 356 ($C_{22}H_{16}N_2O_2$ M^+), 282 ($C_{14}H_{12}N_2O_3$ M^{+2}), 149 ($C_9H_5O_2$ M^{+4}),125 ($C_{10}H_7$ M-2), 84 ($C_3H_4N_2O_1$ M^+), 72 ($C_2H_3O_1N_2$ M^{+1})

3.2.12. Characterizations of 2-(1,3-dioxo-2H-inden-2-yl)-N'-[(Z)- phenylmethylidene] acetohydrazide (AKS12)

71% yield, Ash brown colour, MP: 252-258ºC, Rf value: 0.64, FT-IR (cm^{-1}): 3444.39 (N-H str),2971.19 (CH_2 str), 2880.6 (C-H str), 2323.74 (C=N str), 1670.5 (C=O str), 1614.75 (NH-C=O str), 1527.59 (C=C str Ar). ^{1}H NMR (400MHZ, DMSO): δ ppm 9.9 (s, 1H, NH), 7.4(m, 4H, Ar-H), 7.6 (m, 5H, Ar-H), 7.1 (s, 1H, CH), 2.7 (d, 2H, CH_2), 1.2 (t, 1H, CH).^{13}C NMR (400MHZ, DMSO): δppm 39.36 (CH_2), 50.32 (CH), 120-135 (Ar C), 142.19 (CH), 157.23 (C=O), 195, 200 (Ar C=O). Mass (m/z) – 306($C_{18}H_{14}N_2O_2$ M^+), 218 ($C_{11}H_8N_2O_1$ M^{+2}), 159 ($C_9H_9N_2O_1$ M^{-2}), 141 ($C_9H_5O_2$ M^{-4}), 123 ($C_7H_7N_2$ M^{+4}), 84 ($C_3H_4N_2O_1$ M^{+2}).

Table 6. *Physical data of synthesized compounds*

Compounds	Formula	Mol weight	% yield	Melting point (℃)	Rf value**	Colour
AKS1	$C_{20}H_{18}N_2O_4$	350.37	81	220-225	0.52	Dark Brown
AKS2	$C_{19}H_{15}BrN_2O_3$	399.24	86	230-235	0.36	Light Brown

AKS3	$C_{16}H_{13}N_3O_3S$	327.36	75	242-246	0.22	Ash Brown
AKS4	$C_{16}H_{12}N_2O_4$	296.28	68	215-220	0.42	Brownish black
AKS5	$C_{17}H_{13}N_3O_3$	307.30	65	250-255	0.64	Tan brown
AKS6	$C_{18}H_{13}N_3O_5$	351.31	80	247-252	0.40	Yellowish brown
AKS7	$C_{18}H_{13}N_3O_5$	351.31	86	255-260	0.28	Brown
AKS8	$C_{18}H_{13}Cl_1N_2O_3$	340.76	82	222-227	0.54	Dark Brown
AKS9	$C_{18}H_{14}N_2O_4$	322.31	77	240-245	0.38	Purple brown
AKS10	$C_{18}H_{13}Cl_1N_2O_3$	340.76	79	237-242	0.22	Brownish black
AKS11	$C_{22}H_{16}N_2O_3$	356.38	84	235-240	0.42	Greyish brown
AKS12	$C_{18}H_{14}N_2O_3$	306.32	71	252-258	0.64	Black Brown
Rf value petroleum ether : ethyl acetate solvent system (4:1)**						

The presented **Table 6.** outlines the characteristics of various synthesized compounds, each identified by a specific code (AKS1 to AKS12). These compounds encompass diverse molecular formulas, molecular weights, yields, melting points, Rf values, and colors, offering a rich spectrum of chemical properties for analysis and interpretation. Notably, AKS1 to AKS12 exhibit distinct features. AKS1, AKS2, and AKS3, for instance, demonstrate different molecular formulas and molecular weights, with AKS1 being the most massive among them. Moreover, variations in the yields of these compounds suggest differences in their synthesis efficiency, with AKS2 exhibiting the highest yield at 86%. Melting points serve as crucial indicators of the thermal stability and purity of compounds. AKS5, with a melting point range of 250-255°C, possesses the highest melting point among the compounds listed, indicating its

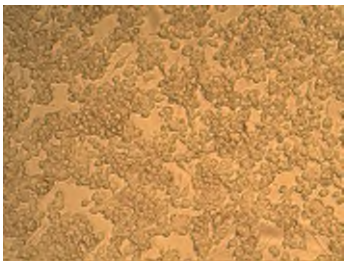
relatively high thermal stability. Contrastingly, AKS4, with a melting point range of 215-220°C, exhibits a lower thermal stability compared to others. The Rf values, determined using a petroleum ether : ethyl acetate solvent system (4:1), provide insights into the compounds' polarity and chromatographic behaviour. For instance, AKS5, with an Rf value of 0.64, indicates a higher polarity compared to AKS3, which has an Rf value of 0.22, suggesting different degrees of interaction with the chromatography matrix. Additionally, the color of the compounds ranges from dark brown (AKS1) to tan brown (AKS5) to greyish brown (AKS7 and AKS11), reflecting variations in their electronic structures and possibly their optical properties. In summary, the characterization data presented offer a comprehensive understanding of the synthesized compounds, laying the groundwork for further exploration of their chemical reactivity, biological activities, and potential applications in various fields such as medicinal chemistry.

3.3. *In-vitro* results

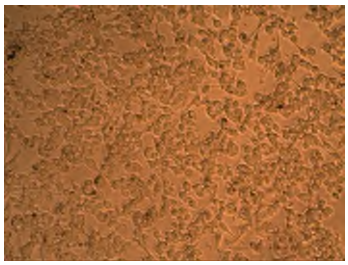
3.3.1. Cell viability Assay by MTT

Based on the results of the cell viability assay shown in **Table 7.** our synthesized compound showed promising results in terms of being non-toxic to the cells. The percentage of cell viability was calculated by comparing the absorbance values of the cells treated with different concentrations of the compound to the control cells that were not treated with the compound. The images obtained were analyzed for any changes in cell morphology, such as changes in cell shape, size, and texture. Any detectable changes, such as cell rounding, shrinkage, or the presence of granules or vacuoles in the cytoplasm, were considered indicators of cytotoxicity. It was found that the cells treated with the synthesized compounds appeared to be similar in morphology to the control cells like circular and fibroblastic in nature, indicating that the compounds did not cause any significant cytotoxicity or changes in cell morphology which is shown in **Figure 4.** The results showed that the cells treated with our compound at

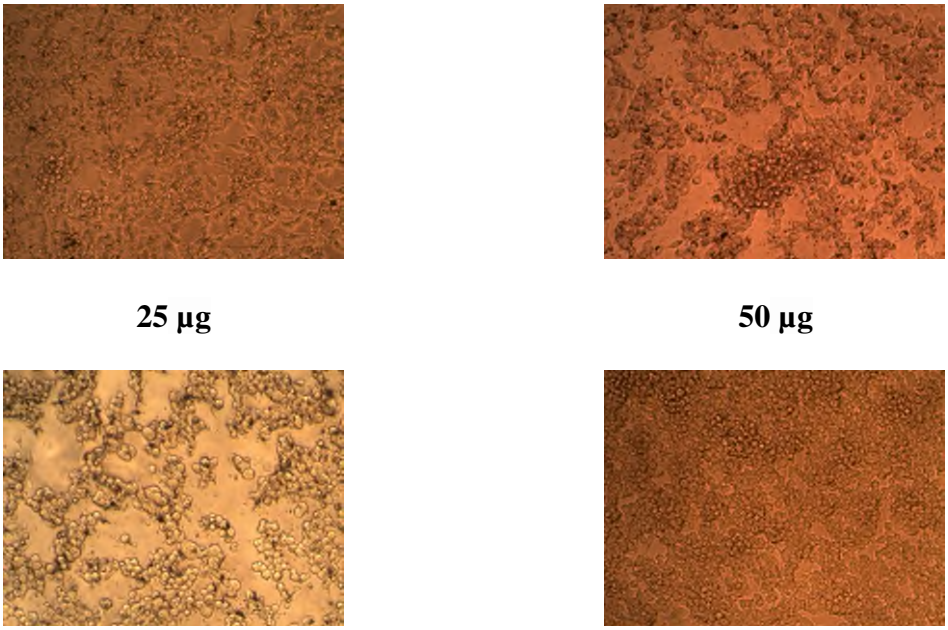
concentrations of 6.25 µg/mL, 12.5 µg/mL, and 25 µg/mL had percentage cell viabilities of 96.9%, 93%, and 84 %, respectively. At higher concentrations of 50 µg/mL and 100 µg/mL, the percentage cell viabilities were 77.95% and 67.84%, respectively. Overall, the results indicate that our synthesized compound is non-toxic to the cells at concentrations up to 25 µg/mL, and has moderate toxicity at higher concentrations. However, the compound is still non-toxic at lower concentrations, which is a positive indication for its use in further studies. The MTT assay is a widely used and reliable method for evaluating cell viability, and the results obtained from this study provide a basis for further investigation of the cytotoxicity and potential therapeutic applications of the synthesized compound. Based on the results of the cell viability assay shown in **Figure 5**, we can conclude that our synthesized compound, with sample code AKS11, is non-toxic to the tested cells. The percentage of cell viability for all the tested concentrations of AKS11 was above 67%, indicating that the compound did not significantly affect the viability of the cells. The IC_{50} value, which represents the concentration of the compound that inhibits 50% of cell growth, was calculated as 153.75 µg/mL using ED_{50} PLUS V1.0 software. This value suggests that the compound has a relatively low cytotoxicity toward the tested cells. These results are promising and indicate that further investigation of the potential therapeutic properties of this compound could be worthwhile.



6.25 µg



12.5 µg



25 µg **50 µg**

100 µg **Control**

Figure 4. *Cell viability Assay by Direct Microscopic observation at different concentrations by AKS11 on RAW264.7 cell lines*

Table 7. *MTT Assay Results for Compound AKS11 at Different Concentrations*

Sample Concentration (µg/mL)	OD value I	OD value II	OD value III	Average OD	Percentage Viability (%)
Control	0.8024	0.8125	0.8114	0.8088	100.00
Sample code: AKS11					
6.25	0.785	0.7754	0.7837	0.7814	96.90
12.5	0.7415	0.7405	0.7522	0.7447	93.00
25	0.6925	0.6934	0.684	0.6900	84.57
50	0.6412	0.6312	0.6305	0.6343	77.95
100	0.5434	0.5565	0.5487	0.5495	67.84

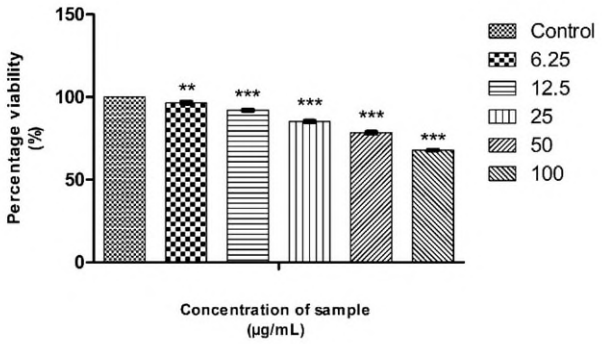


Figure 5. *Graphical representation depicting the cytotoxic effect of AKS11 on RAW 264.7 cells by MTT assay. ***p < 0.001 compared to control groups, **p < 0.01 compared to control groups.*

3.3.2. Indirect ELISA

Table 8. shows the results of an indirect ELISA assay conducted to evaluate the inhibitory activity of synthesized compounds on the production of Interleukin-6 (IL-6) in Raw264.7 cells. The cells were treated with lipopolysaccharide (LPS) to induce IL-6 production and then exposed to the synthesized compounds and a standard drug (methotrexate) at a concentration of 25 µg/mL. The Indirect ELISA assay was performed to evaluate the inhibitory activity of synthesized compounds (AKS1 to AKS12) on the production of Interleukin-6 (IL-6) protein. The table shows the absorbance values at 415 nm, protein concentration, and activity units/mg protein for each sample. **Figure 6**, shows the comparison of results through bar diagram representation. AKS7 and AKS11 had the highest inhibitory activity with activity units/mg protein of 1.2553 and 1.3947, respectively. This means that these compounds were able to inhibit the production of IL-6 more effectively compared to the LPS control group and the standard drug methotrexate, which had activity units/mg protein of 3.7208 and 1.6548, respectively. On the other hand, AKS12 had the lowest inhibitory activity among all compounds with an activity units/mg protein of 2.8133, which is higher than the activity of methotrexate. The remaining compounds (AKS1 to AKS6, AKS8 to AKS10) had moderate inhibitory activity on the production of IL-6 with activity units/mg protein ranging from 1.559

to 2.1075. It is important to note that the inhibitory activity of a compound is dependent on its concentration. The concentration used in this study was 25 µg/mL, which was determined to be the optimal dose based on the cell viability assay. Therefore, some compounds may have had higher inhibitory activity at a higher concentration. AKS7 and AKS11 had the lowest concentration of IL-6 compared to LPS and methotrexate, indicating that they have a higher potential to inhibit the production of this pro-inflammatory cytokine. This is supported by the higher percentage inhibition values for IL-6 in AKS7 (66.26%) and AKS11 (61.54%) compared to LPS (0%) and methotrexate (55.52%). The percentage inhibition value indicates the degree to which the test compounds (AKS7, AKS11, methotrexate) can inhibit the production of IL-6 compared to the control (LPS). In this case, a higher percentage inhibition value means that the test compounds are more effective at inhibiting the production of IL-6. AKS7 and AKS11 had the highest percentage inhibition values, indicating that they are more effective at inhibiting the production of IL-6 than methotrexate, which is a known anti-inflammatory drug. Therefore, AKS7 and AKS11 may have potential as anti-inflammatory agents due to their ability to inhibit the production of IL-6. However, further studies are needed to determine their safety and efficacy *in-vivo* before they can be used as therapeutic agents.

Table 8. *Estimation of LPS induced IL-6 levels in RAW264.7 cell lines by indirect Elisa.*

Sample code	Absorbance at 415nm	Protein concentration	Activity Units/mg protein	Percentage inhibition (%)
AKS7	0.8098	0.6451	1.2553	66.26283
AKS11	0.7275	0.5084	1.4309	61.54212
AKS5	0.6481	0.4156	1.5594	58.08935
AKS6	0.8262	0.5131	1.6102	56.7246

AKS9	0.8505	0.5216	1.6305	56.17776
STANDARD DRUG METHOTREXATE	0.8180	0.4943	1.6548	55.52453
AKS10	0.7853	0.4713	1.6662	55.21877
AKS1	0.9334	0.4769	1.9572	47.39847
AKS2	0.8490	0.4242	2.0014	46.21082
AKS3	0.8751	0.4341	2.0158	45.82165
AKS4	0.8717	0.4296	2.0290	45.46684
AKS8	1.0094	0.4522	2.2321	40.00838
AKS12	1.2041	0.4280	2.8133	24.39045
CONTROL (LPS)	1.6115	0.4331	3.7208	0

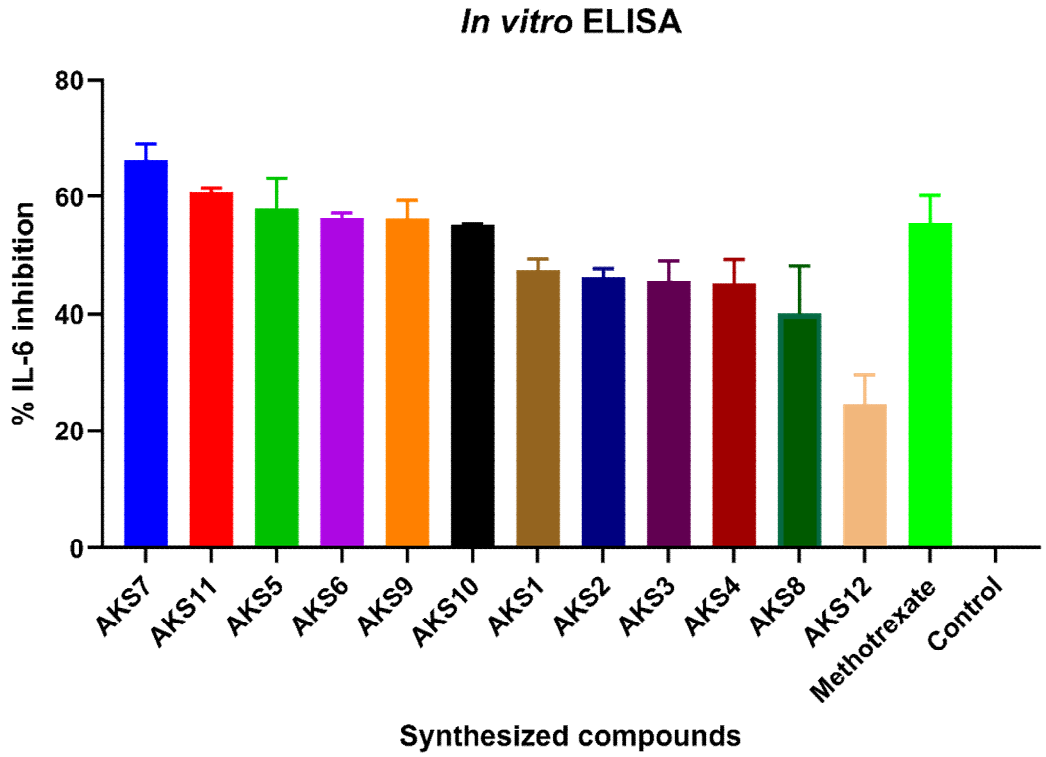


Figure 6. *Graphical representation depicting the LPS induced IL-6 inhibition by AKS11 on RAW 264.7 cells by Indirect Elisa.*

3.3.3. RTPCR Results:

Table 9. *Mean Ct Values of IL-6 gene in RAW264.7 Cell line*

Samples	IL-6				GAPDH			
	Ct1	Ct2	Ct3	Ct Mean	Ct1	Ct2	Ct3	Ct Mean
Control	24.98	24.94	24.97	24.98	16.52	19.68	19.51	18.57
LPS	23.59	28.12	23.63	25.11	18.19	17.80	17.85	17.95
AKS7	24.72	25.22	25.16	25.03	18.61	18.55	18.90	18.69
AKS11	22.45	22.45	23.44	22.78	17.35	17.35	17.31	17.34

In this **Table 9.** the Ct values for the IL-6 gene in the RAW264.7 cell line are presented for different samples. The control group shows a mean Ct value of 24.98, indicating moderate expression of the IL-6 gene. The LPS-treated group exhibits a mean Ct value of 25.11, suggesting slightly higher expression compared to the control group. The AKS7 and AKS11 groups show mean Ct values of 25.03 and 22.78, respectively, indicating similar or slightly higher expression compared to the control group. These Ct values provide initial insights into the expression levels of the IL-6 gene in each sample.

Table 10. *ΔΔCt Values of IL-6 gene in RAW264.7 Cell line*

Samples	ΔCt	ΔΔCt	2^-(ΔΔCt)
Control	6.41	0	0
LPS	7.17	0.76	0.589814556
AKS7	6.35	-0.06	1.044877153
AKS11	5.44	-0.96	1.947558504

Table 10. presents the ΔΔCt values, which indicate the relative change in gene expression compared to the control group. The control sample serves as the reference with a ΔΔCt value of 0. The LPS-treated group shows a ΔΔCt value of 0.76, indicating a 0.589-fold increase in

gene expression compared to the control. The AKS7 group exhibits a ΔΔCt value of -0.06, suggesting a slight decrease (-0.0448-fold change) in gene expression compared to the control. The AKS11 group shows a ΔΔCt value of -0.96, indicating a significant decrease (-0.9475-fold change) in gene expression compared to the control. These values provide insights into the relative changes in IL-6 gene expression in each sample.

Table 11. *Relative Gene Expression of IL-6 gene*

Samples	**Control**	**Samples**
Control	1	–
LPS	1	1.5898
AKS7	1	-0.0448
AKS11	1	-0.9475

Table 11. presents the relative gene expression values for the IL-6 gene compared to the control group. The control sample is assigned a value of 1 to represent the baseline expression level. The LPS-treated group shows a relative gene expression value of 1.5898, indicating an upregulation of the IL-6 gene compared to the control. The AKS7 group exhibits a relative gene expression value of -0.0448, suggesting downregulation of the IL-6 gene compared to the control. Similarly, the AKS11 group shows a relative gene expression value of -0.9475, indicating significant downregulation of the IL-6 gene compared to the control. These relative gene expression values provide insights into the fold change in IL-6 gene expression in each sample compared to the control group which is shown in **Figure 7**, and further evidenced by Agarose gel electrophoresis bands shown in **Figure 8.**

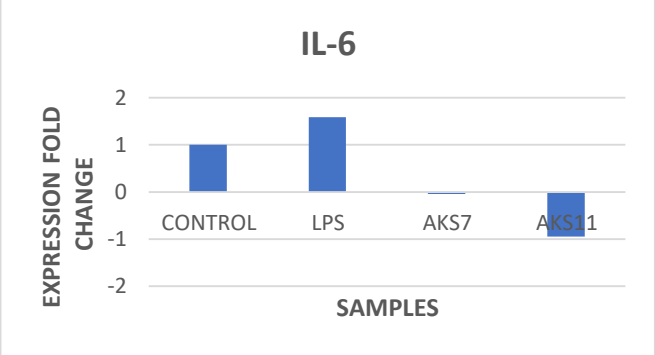


Figure 7. *Graphical representation depicting the relative gene expression pattern of IL6 by AKS 7&11 on RAW 264.7 cells by RT-PCR method.*

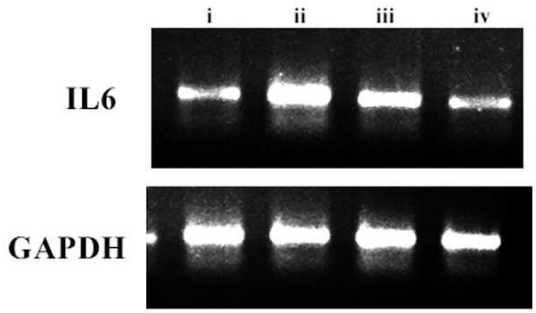


Figure 8. *Agarose gel electrophoresis Lane-I- control, Lane II- LPS, Lane III- LPS+7, Lane IV- LPS+11.*

Based on the comprehensive *in-vitro* evaluations conducted, our novel compounds demonstrate promising characteristics as inhibitors of both IL-6 protein expression and IL-6 mRNA gene expression. Regarding IL-6 protein inhibition, the results from the indirect ELISA assay indicate significant inhibitory activity of several synthesized compounds, particularly AKS7 and AKS11, on the production of IL-6 protein in RAW264.7 cells. These compounds exhibited higher inhibitory activity compared to the standard drug methotrexate, suggesting their effectiveness in suppressing IL-6 protein expression. Furthermore, the RT-PCR results revealed varying levels of downregulation of the IL-6 gene expression in RAW264.7 cells treated with our synthesized compounds, particularly AKS7 and AKS11. This suggests that these compounds may act as inhibitors of IL-6 mRNA gene expression, thereby further supporting their potential therapeutic utility in modulating IL-6 signaling pathways. In

conclusion, based on these findings, our novel compounds exhibit dual inhibitory activity against both IL-6 protein expression and IL-6 mRNA gene expression. These promising results warrant further investigation into the mechanisms of action and therapeutic potential of these compounds in managing conditions associated with dysregulated IL-6 signaling.

4. *In-vivo* studies

4.1. Acute oral toxicity (OECD 423)

Following acute oral toxicity trials conducted in accordance with OECD 423 guidelines, it was observed that the groups administered 2000 mg/kg of the test compound exhibited no adverse effects, and there were no fatalities recorded. Notably, all mice in the group receiving the 2000 mg/kg dose of the test compound survived throughout the observation period. These findings led to the determination of 100 mg/kg as the high dose and 50 mg/kg as the low dose for further evaluation of pharmacological activity. This outcome underscores the safety profile of the test compound at the administered doses, providing crucial insights for subsequent pharmacological assessments.

4.2. Induction of Arthritis by Complete Freund's adjuvant (CFA)

In this study, arthritis was induced in rats by administering Complete Freund's adjuvant (CFA), containing 1 mg/ml Mycobacterium tuberculosis in mineral oil, into the sub-plantar region of the left hind paw on Day 1 under light anaesthesia. Notably, the morphological changes observed over the 28-day period revealed a marked reduction in arthritis severity across all treatment groups, indicating progressive improvement. Visual evidence of reduced inflammation and improved morphology strongly supports the therapeutic efficacy of the treatment regimen in managing rheumatoid arthritis. Specifically, it is evident from the figure that both the low and high doses of AKS7, as well as the low and high doses of AKS11, exhibit significant improvement compared to the diseased group and the standard methotrexate treatment. This observation underscores the potential effectiveness of AKS7 and AKS11 in

alleviating rheumatoid arthritis symptoms, as indicated by the visual evidence of reduced inflammation and improved joint morphology which is shown in **Figure 9**.



Figure 9. *Morphological Changes after the treatment of rheumatoid arthritis*

4.3. Arthritic Parameters

4.3.1. Paw volume

The paw volume measurements presented in **Table 12.** depict the progression of arthritis in rats over a 28-day period, along with the impact of different treatment interventions. Initially, Group II animals, representing the negative control group, exhibited a significant increase in paw volume compared to the normal control group (Group I) on all observation days ($p<0.05$). This increase reflects the development and progression of arthritis in the untreated group. However, treatment with test drugs and the standard reference (Group III to Group VII) resulted in notable reductions in paw volume compared to the negative control group (Group II) from Day 1 onwards ($p<0.05$). This decrease in paw volume suggests an ameliorative effect of the treatments on arthritis-induced inflammation and swelling. Of particular significance is the substantial reduction in paw volume observed in Group V and Group VII, treated with AKS7

and AKS11 at high doses, respectively, compared to the negative control group (Group II) throughout the study period. These findings underscore the efficacy of AKS7 and AKS11 in mitigating arthritis symptoms, as evidenced by the significant decrease in paw volume which is shown in **Figure 10**.

Table 12. *Morphological changes of Paw volume*

Days	Group I	Group II	Group III	Group IV	Group V	Group VI	Group VII
Day 0	0.18±0.06	0.18±0.06	0.15±0.05	0.16±0.07	0.11±0.06	0.18±0.03	0.20±0.08
Day 1	0.15±0.05	1.65±0.17$^{\#}$	1.51±0.19	1.63±0.28	1.65±0.35	1.55±0.17	1.90±0.13
Day 7	0.15±0.05	1.83±0.23$^{\#}$	1.40±0.21*	1.46±0.24*	1.43±0.38*	1.35±0.19*	1.71±0.15*
Day 14	0.13±0.10	1.95±0.17$^{\#}$	1.23±0.26*	1.25±0.16*	1.26±0.40*	1.21±0.15*	1.41±0.24*
Day 21	0.10±0.0	2.23±0.19$^{\#}$	1.06±0.26*	1.11±0.16*	1.08±0.35*	1.06±0.09*	1.21±0.15*
Day 28	0.13±0.04	2.51±0.13$^{\#}$	0.83±0.16*	1.01±0.16*	0.85±0.30*	0.96±0.11*	0.75±0.12*

Values are Mean± SD, n=6; $^{\#}p< 0.05$ vs Normal control; $^{*}p< 0.05$ vs Negative control, two- way ANOVA followed by Tukey's multiple comparison test.

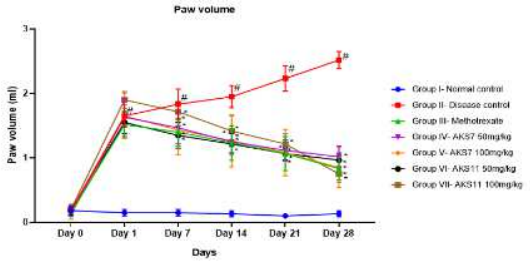


Figure 10. *Paw volume, values are Mean± SD, n=6; $^{\#}p< 0.05$ vs Normal control; $^{*}p< 0.05$ vs Negative control.*

4.3.2. Arthritic score

The arthritic score data provided in **Table 13.** offers insights into the progression of arthritis and the efficacy of various treatment interventions over the 28-day observation period. Initially, Group II animals, representing the negative control group, exhibited a significant increase in arthritic score compared to the normal control group (Group I) on all observation days ($p<0.05$). This rise in arthritic score reflects the development and worsening of arthritis in the untreated group. Conversely, treatment with test drugs and the standard reference (Group III to Group VII) resulted in significant decreases in arthritic score compared to the negative control group (Group II) from Day 1 onwards ($p<0.05$). This reduction in arthritic score suggests a therapeutic effect of the treatments on arthritis severity and progression. Of particular note is the considerable decrease in arthritic score observed in Group V and Group VII, treated with AKS7 and AKS11 at high doses, respectively, compared to the negative control group (Group II) throughout the study period. This finding highlights the pronounced efficacy of AKS7 and AKS11 in mitigating arthritis symptoms, as evidenced by the significant decrease in arthritic score which is shown in **Figure 11.**

Table 13. *Morphological changes of Arthritic score*

Days	Group I	Group II	Group III	Group IV	Group V	Group VI	Group VII
Day 0	0±0	1.0±0.0	1.0±0.0	1.0±0.0	1.0±0.0	1.0±0.0	1.0±0.0
Day 1	0±0	1.83±0.37$^{\#}$	1.66±0.47	1.50±0.50	1.33±0.47	1.50±0.50	1.33±0.47
Day 7	0±0	3.0±0.0$^{\#}$	2.0±0.0*	1.66±0.47*	2.66±0.47*	2.33±0.74*	2.0±0.0*
Day 14	0±0	3.0±0.0$^{\#}$	2.0±0.0*	1.66±0.47*	1.83±0.37*	1.16±0.89*	1.50±0.50*
Day 21	0±0	3.0±0.0$^{\#}$	1.33±0.47*	1.50±0.50*	1.66±0.47*	1.0±0.57*	1.0±0.0*
Day 28	0±0	3.0±0.0$^{\#}$	0.66±0.47*	1.50±0.50*	0.66±0.47*	0.50±0.50*	0.66±0.47*

Values are Mean± SD, n=6; $^{\#}p< 0.05$ vs Normal control; $^{*}p< 0.05$ vs Negative control, two- way ANOVA followed by Tukey's multiple comparison test.

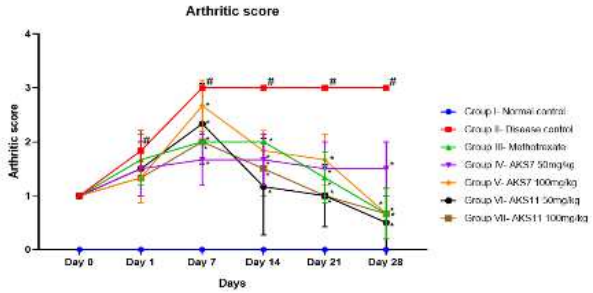


Figure 11. *Arthritic score, values are Mean± SD, n=6; $^{\#}p< 0.05$ vs Normal control; $^{*}p< 0.05$ vs Negative control.*

4.3.3. Morphological changes of Body weights

The body weight data presented in **Table 14.** indicates that there were no significant changes in body weight observed across all treatment groups throughout the study period. Comparing the body weights of animals in Group II (negative control) with those in Group I (normal control), there were no statistically significant differences noted on any of the observation days ($p<0.05$). Similarly, no significant variations in body weight were observed among the groups treated with test drugs (Group III to Group VII) and the standard reference compared to the negative control group (Group II) across all observation days ($p<0.05$). These findings suggest that the administration of the test drugs and the standard reference did not induce any notable alterations in body weight in the experimental animals. The consistent body weight values observed in all groups throughout the study duration indicate that the treatments did not exert any discernible adverse effects on the overall health or growth of the animals. This stability in body weight further supports the safety profile of the test drugs and the standard reference at the administered doses. Overall, the lack of significant changes in body weight across all treatment groups underscores the absence of systemic toxicity or metabolic disturbances associated with the test drugs and the standard reference, reaffirming their potential suitability for further evaluation in preclinical and clinical studies for arthritis management which is shown in **Figure 12.**

Table 14. *Morphological changes of Body weight (g)*

Days	Group I	Group II	Group III	Group IV	Group V	Group VI	Group VII
Day 0	201.6±16.2	177.5±12.5	193.3±20.3	205.2±20.1	233.8±21.2	216.3±17.1	206.2±10.5
Day 1	209.8±17.2	178.0±12.5	193.6±21.4	205.5±22.4	231.0±15.7	220.6±14.9	212.5±15.7
Day 7	214.3±15.3	193.0±17.8	199.2±18.8	208.0±25.3	243.5±20.2	220.2±15.7	241.3±30.5
Day 14	217.2±12.2	197.5±18.7	199.2±27.3	205.2±21.8	247.8±20.3	227.2±13.9	245.2±27.9
Day 21	221.3±6.7	206.8±20.3	196.5±35.4	213.2±21.3	249.5±17.5	232.8±17.5	254.3±28.7
Day 28	223.2±7.3	213.3±20.2	195.2±46.8	218.2±22.2	246.5±6.7	238.2±19.4	255.0±39.8

Values are Mean± SD, n=6; $^{\#}p< 0.05$ vs Normal control; $^{*}p< 0.05$ vs Negative control, two- way ANOVA followed by Tukey's multiple comparison test.

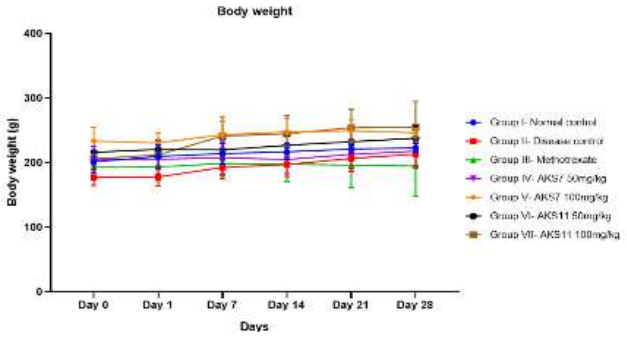


Figure 12. *Body weight, values are Mean± SD, n=6; $^{\#}p< 0.05$ vs Normal control; $^{*}p< 0.05$ vs Negative control.*

4.4. Histopathological analysis of ankle joints

The histopathological analysis of ankle joints revealed significant improvements in joint architecture and reduction in inflammatory cell infiltration in treatment groups compared to the disease control. Treatment with AKS7 and AKS11 exhibited dose-dependent improvements in joint space and reduction in cellular infiltration, indicating their potential therapeutic efficacy in mitigating rheumatoid arthritis-induced joint damage which show therapeutic potential and histological improvement which is shown in **Figure 13**.

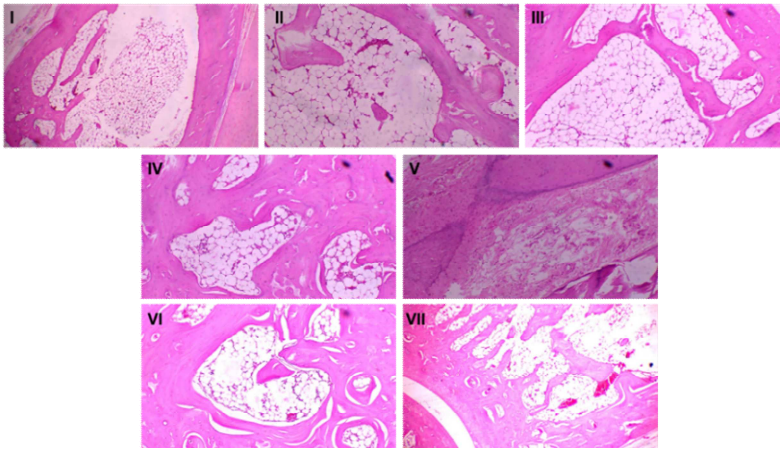


Figure 13. *Histopathological images.*

4.5. Estimation of IL-6 by Indirect ELISA in *in-vivo*

Table 15. IL-6 inhibition by Indirect Elisa in plasma

Sample code	Absorbance at 415nm	Protein concentration	Activity Units/mg protein	Percentage inhibition (%)
Control	0.1213	1.162651	0.104335	45.47967539
Disease control	0.2071	1.082242	0.191369	0
Methotrexate	0.1239	1.251702	0.098985	48.2753215
AKS7 (Low dose)	0.127	1.320587	0.096176	49.74316634
AKS7 (High dose)	0.1115	1.354636	0.082312	56.98780889

AKS11 (Low dose)	0.1489	1.509167	0.098668	48.44097006
AKS11 (High dose)	0.0944	1.093243	0.086352	54.87670417

Table 15. shows the results of the IL-6 inhibition by Indirect ELISA in plasma provide valuable insights into the effectiveness of the synthesized compounds in modulating IL-6 levels *in-vivo*. In the control group, the absorbance at 415nm was recorded at 0.1213, with a corresponding protein concentration of 1.162651 mg/ml. This translated to an activity of 0.104335 units/mg protein and a percentage inhibition of 45.48%. Conversely, the disease control group exhibited significantly elevated IL-6 levels, as indicated by an absorbance of 0.2071 and a protein concentration of 1.082242 mg/ml. However, the activity units/mg protein were notably lower at 0.191369, reflecting minimal inhibition of IL-6 production. Administration of the standard drug methotrexate resulted in a reduction in IL-6 levels, with an absorbance of 0.1239 and a protein concentration of 1.251702 mg/ml. This translated to an activity of 0.098985 units/mg protein and a percentage inhibition of 48.28%. Furthermore, treatment with AKS7 and AKS11 at both low and high doses demonstrated promising inhibitory effects on IL-6 production. AKS7, administered at low and high doses, exhibited absorbance values of 0.127 and 0.1115, respectively, with corresponding protein concentrations and activity units/mg protein indicating significant percentage inhibitions of 49.74% and 56.99%, respectively. Similarly, AKS11, at low and high doses, showed absorbance values of 0.1489 and 0.0944, respectively, with corresponding protein concentrations and activity units/mg protein indicating percentage inhibitions of 48.44% and 54.88%, respectively which is shown in **Figure 14**. Overall, these findings suggest that both AKS7 and AKS11 effectively attenuate IL-6 levels in plasma, with higher doses resulting in greater inhibition. These results support the potential therapeutic utility of these compounds in mitigating inflammatory processes associated with conditions such as rheumatoid arthritis.

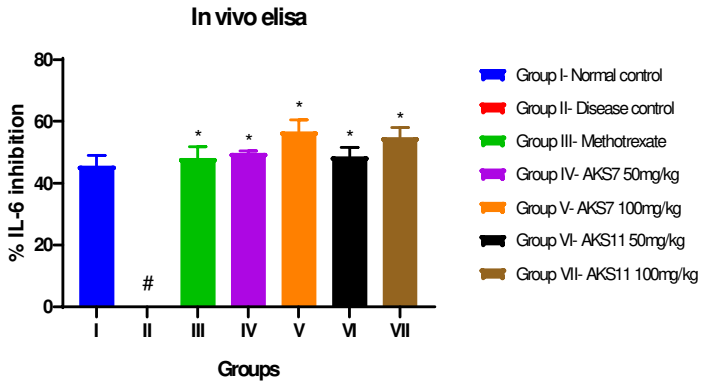


Figure 14. *In-vivo ELISA (Values are Mean± SD, n=3; $^{\#}p< 0.05$ vs Normal control; $^{*}p< 0.05$ vs Negative control.*

4.6. RTPCR Results:

Table 16. *Mean Ct Values of IL-6 & STAT-3 genes in tissue*

Samples	IL-6				STAT-3				GAPDH			
	Ct1	Ct2	Ct3	Ct Mean	Ct1	Ct2	Ct3	Ct Mean	Ct1	Ct2	Ct3	Ct Mean
Control	32.71	33.10	32.38	32.73	30.32	35.08	36.12	33.84	24.73	25.79	25.18	25.23
Disease control	23.71	24.54	24.41	24.22	26.43	26.01	25.92	26.12	18.10	16.23	15.51	16.61
Methotrexate	34.97	34.10	34.39	34.49	33.88	38.39	33.88	35.38	23.76	25.85	29.25	26.29
AKS7	22.72	23.20	22.51	22.81	22.85	22.86	22.80	22.84	16.40	15.23	15.33	15.65
AKS11	30.75	31.24	31.65	31.21	29.39	33.61	33.61	32.20	24.54	24.21	24.65	24.47

Table 17. *ΔΔCt Values of IL-6 gene and STAT-3 gene in RAW264.7 Cell line*

Samples	IL-6 gene			STAT-3 gene		
	ΔCt	ΔΔCt	2^-(ΔΔCt)	ΔCt	ΔΔCt	2^-(ΔΔCt)
Control	7.50	0	0	8.61	0	0
Disease control	7.61	0.11	0.926588062	9.51	0.90	0.535886731
Methotrexate	8.20	0.70	0.614151575	10.67	2.07	0.238710401

AKS7	7.16	-0.34	1.265756594	7.18	-1.42	2.682044796
AKS11	6.75	-0.75	1.681792831	7.74	-0.87	1.8276629

Table 18. *Relative Gene Expression of IL-6 & STAT-3 genes in tissue*

Samples	**Control**	**IL-6 Gene Samples**	**STAT-3 Gene Samples**
Control	1	–	-
Disease control	1	1.926581	1.535886731
Methotrexate	1	1.6142	1.238710401
AKS7	1	-0.26576	-1.682044796
AKS11	1	-0.68179	-0.827629

Table 16, says, In the control group, the mean Ct values for IL-6 and STAT-3 genes are relatively higher, indicating moderate expression levels. GAPDH, the reference gene, shows stable and abundant expression. The disease control group exhibits significantly lower mean Ct values for IL-6 and STAT-3 genes compared to the control, indicating upregulated gene expression in response to the disease condition. Methotrexate treatment shows comparable mean Ct values to the control group, suggesting minimal impact on gene expression. AKS7 and AKS11 treatments demonstrate variations in gene expression levels compared to the control and disease control groups, potentially indicating regulatory effects of the compounds.

Table 17, presents, ΔΔCt values represent the relative change in gene expression compared to the control group. Negative values indicate downregulation, while positive values indicate upregulation. Disease control and Methotrexate groups show positive ΔΔCt values, indicating upregulated expression of IL-6 and STAT-3 genes. AKS7 and AKS11 groups exhibit negative ΔΔCt values for both genes, suggesting downregulation or inhibition of gene expression by the compounds.

Table 18, presents, relative gene expression values represent fold changes compared to the control group. In the disease control and Methotrexate groups, both IL-6 and STAT-3 genes show increased fold expression compared to the control. AKS7 and AKS11 groups exhibit decreased fold expression of both IL-6 and STAT-3 genes, indicating potential inhibitory effects of the compounds on the expression of these genes which is shown in **Figure 15 & 16**, and further evidenced by Agarose gel electrophoresis bands shown in **Figure 17**.

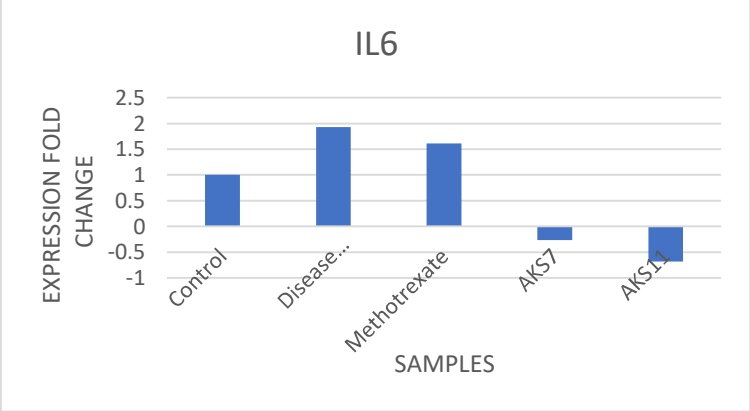


Figure 15. *Graphical representation depicting the relative gene expression pattern of IL-6 by AKS11 on animal bone tissue by RT-PCR method.*

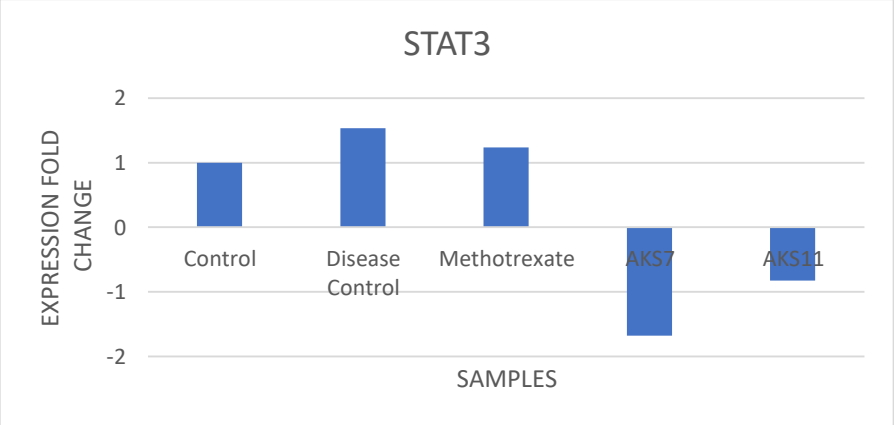


Figure 16. *Graphical representation depicting the relative gene expression pattern of STAT-3 by AKS11 on animal bone tissue by RT-PCR method.*

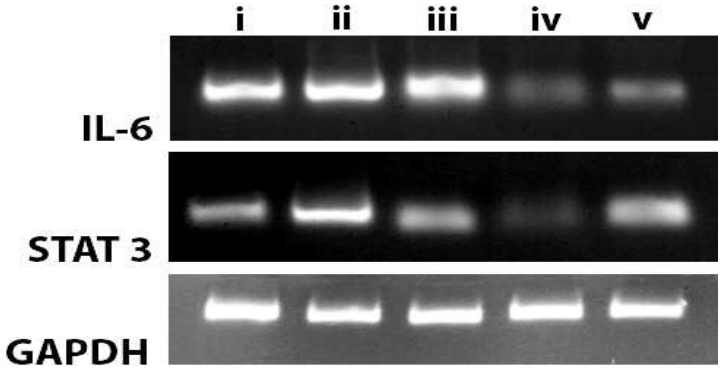
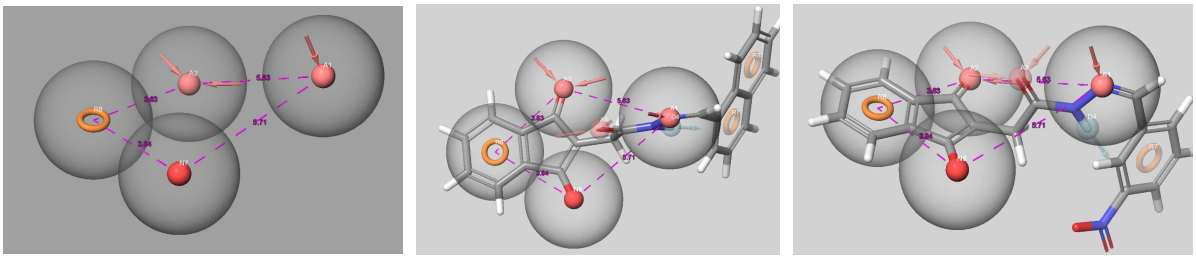


Figure 17. *Agarose gel electrophoresis Lane-I- control, Lane II- disease control, Lane III- methotrexate, Lane IV- AKS7, Lane IV- AKS11*

Based on the extensive *in-vivo* studies conducted, our novel compounds demonstrate significant potential as inhibitors of both IL-6 protein expression and IL-6 mRNA gene expression, as well as STAT-3 gene expression. The results from the indirect ELISA assay revealed notable inhibitory activity of several synthesized compounds, particularly AKS7 and AKS11, on the production of IL-6 protein in plasma. These compounds exhibited higher inhibitory activity compared to the standard drug methotrexate, indicating their efficacy in suppressing IL-6 protein expression *in-vivo*. Furthermore, the RT-PCR results demonstrated varying degrees of downregulation in the expression of the IL-6 gene in animal tissues treated with our synthesized compounds, with AKS7 and AKS11 showing particularly significant effects. Additionally, the evaluation of STAT-3 gene expression provided further insights into the potential mechanism of action of these compounds, suggesting their ability to modulate the IL-6/STAT-3 signaling pathway. In conclusion, based on these findings, downregulation of STAT-3 gene expression suggests that our novel synthesized compounds AKS11 and AKS7 are likely inhibiting IL-6 mRNA gene expression. Additionally, the inhibitory effects observed on both IL-6 protein expression and IL-6 mRNA gene expression further support the notion that these compounds possess dual inhibitory actions on the IL-6 signaling pathway. Therefore, it may be concluded that the compounds have the potential to effectively modulate IL-6-mediated inflammation through their actions on both IL-6 protein and mRNA expression, as well as STAT-3 gene expression, making them promising candidates for further development as therapeutic agents for conditions associated with dysregulated IL-6/STAT-3 signaling pathways.

5. Proposed pharmacophore hypothesis



Generated Pharmacophore *AKS11* *AKS7*

Figure 18. *Proposed pharmacophore model for designed molecules*

The proposed pharmacophore hypothesis, derived from the synthesized molecules, comprises four essential structural elements. These elements include an aromatic ring, two hydrogen bond acceptors, and one negatively charged ion which is shown in **Figure 18**. Such a pharmacophore is meticulously designed to ensure optimal binding affinity and inhibitory activity of the molecules towards the IL-6 receptor. The presence of an aromatic ring within the pharmacophore framework suggests a crucial role in facilitating interactions with specific binding sites on the IL-6 receptor, thereby enhancing the overall binding affinity of the molecules. Additionally, the incorporation of two hydrogen bond acceptors further enhances the potential for forming critical hydrogen bonds with complementary functional groups on the receptor surface. This interaction is pivotal for stabilizing the ligand-receptor complex and mediating inhibitory effects on IL-6 signaling pathways. Moreover, the inclusion of a negatively charged ion within the pharmacophore architecture provides an additional layer of specificity in ligand-receptor interactions. This feature likely contributes to electrostatic interactions with positively charged residues on the receptor surface, further strengthening the binding affinity and inhibitory potency of the molecules. Overall, the meticulous arrangement of these key structural elements within the proposed pharmacophore underscores their collective importance in dictating the inhibitory activity of the molecules towards the IL-6 receptor. By targeting specific molecular features essential for effective receptor binding, the

pharmacophore hypothesis serves as a valuable guiding framework for the rational design and optimization of novel therapeutic agents targeting IL-6-mediated pathological conditions.

6. Proposed SAR

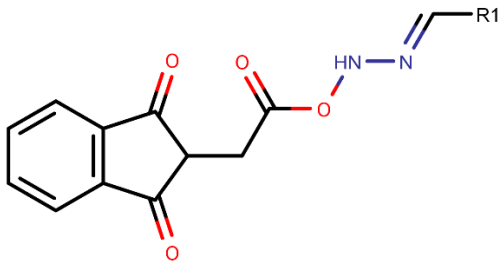


Figure 19. *Proposed SAR for designed compounds.*

i. Hypothesis 1: The presence of 1,3-indanedione may contribute significantly to the IL-6 inhibitory activity.

ii. Hypothesis 2: The two keto groups of the 1,3-indanedione moiety can act as hydrogen bond acceptors with suitable hydrogen bond donors on the target protein potentially.

iii. Hypothesis 3: Electron-Withdrawing Groups (EWGs) on the Benzylidene Moiety (R1) enhance the IL-6 inhibitory activity.

iv. Hypothesis 4: Position of the EWG on the Benzylidene Moiety (R1) at meta position increases the activity.

v. Hypothesis 5: Electron-Donating Groups (EDGs) on the Benzylidene Moiety (R1) may decrease the activity which are shown in **Figure 19.**

7. Summary

Identifying IL-6 dysregulation as a key factor in chronic inflammation and autoimmune disorders, our research emphasizes the need for novel small molecule inhibitors targeting IL-6. In pursuit of this, we explored 1,3-indanedione as a potential IL-6 inhibitor, employing bioisosterism to enhance compound design. Our pharmacogenomic studies involved a comprehensive analysis of 3600 Single Nucleotide Polymorphisms (SNPs) associated with IL-6, revealing that approximately 66% were missense variants impacting protein function. We

identified critical amino acid residues within the IL-6 protein structure essential for ligand binding, guiding the rational design of inhibitors targeting specific binding sites. This led to the identification of 12 mutations within the IL-6 protein's binding sites, underscoring the influence of genetic variations on protein structure and function, which is crucial for understanding inhibitor efficacy and specificity. Proteomics analysis using the Ramachandran plot confirmed that both wild-type and mutated IL-6 proteins exhibit structural integrity and flexibility, making them suitable for binding interactions with the designed 1,3-indanedione derivatives. Molecular docking simulations demonstrated robust binding affinities of AKS11 and AKS7 towards both wild-type and mutated IL-6 proteins, indicating their potential efficacy against various IL-6 variants. These findings were further supported by MMGBSA analysis, which revealed consistently low binding free energies for AKS11 and AKS7, suggesting their suitability as potent therapeutic agents for IL-6-related disorders. ADMET analysis of AKS11 and AKS7 showed favorable drug-like properties, emphasizing their safety profiles and pharmacokinetic characteristics, essential for further drug development and clinical translation. The synthesis of twelve compounds followed a sequential process, beginning with a C-alkylation reaction between 1,3-indanedione and ethyl chloroacetate to yield ethyl 2-(1,3-dioxo-2H-inden-2-yl) acetate, followed by hydrazone formation, ensuring reproducibility. The final compounds, AKS1 to AKS12, were characterized by unique spectroscopic data, including FT-IR, 1H and 13C NMR spectra, and mass spectra. MTT assays demonstrated non-toxicity of our synthesized compounds up to a 25 µg/mL dose, indicating a safe dosage for further studies. *In-vitro* evaluations revealed significant inhibition of IL-6 protein expression by compounds AKS7 and AKS11, surpassing methotrexate's efficacy. RT-PCR analysis showed downregulation of IL-6 gene expression by AKS7 and AKS11, indicating inhibition of IL-6 mRNA. Our novel compounds exhibit dual inhibitory activity against both IL-6 protein and mRNA expression, suggesting therapeutic potential in managing IL-6-related conditions.

Acute oral toxicity trials confirmed the safety profile of the test compounds, with no adverse effects observed at a dose of up to 2000 mg/kg. Treatment with AKS7 and AKS11 led to a marked reduction in arthritis severity, evidenced by reduced inflammation and improved joint morphology, along with notable reductions in paw volume, arthritic scores, body weight, and positive histopathological outcomes. *In-vivo* studies demonstrated significant potential of AKS7 and AKS11 as inhibitors of IL-6 protein, IL-6 mRNA, and STAT-3 gene expression in animal tissues, suggesting their potential therapeutic utility in managing conditions associated with dysregulated IL-6/STAT-3 signaling pathways. The proposed pharmacophore hypothesis for IL-6 receptor inhibition emphasizes key structural elements, including an aromatic ring, two hydrogen bond acceptors, and one negatively charged ion, optimizing binding affinity. Specific Structure-Activity Relationship (SAR) hypotheses highlight the importance of the 1,3-indanedione core and keto groups as hydrogen bond acceptors, and the influence of electron-withdrawing and donating groups on the Benzylidene Moiety (R1) position. These insights facilitate the rational design and optimization of novel IL-6 inhibitors, advancing the development of potent therapeutic agents targeting IL-6-mediated pathways.

Discussion:

Our research represents a significant advancement in IL-6 inhibition by introducing a novel approach utilizing 1,3-indanedione derivatives. Unlike previous studies, which often focused on conventional small molecules or monoclonal antibodies, our approach integrates bioisosterism to enhance the design and efficacy of IL-6 inhibitors. By conducting a thorough pharmacogenomic analysis, we identified critical amino acid residues and mutations in the IL-6 protein that are crucial for ligand binding. This information guided the rational design of our compounds, resulting in novel inhibitors with targeted interactions. The dual inhibitory activity of our compounds against both IL-6 protein and mRNA expression is an innovative aspect, potentially offering a more comprehensive therapeutic approach compared to existing

therapies. Our compounds, specifically AKS7 and AKS11, exhibit superior efficacy and safety profiles, marking a notable advancement in the field of IL-6-targeted therapies.

The IL-6 inhibitory activity of our compounds can be attributed to several key factors. Firstly, the rational design of our 1,3-indanedione derivatives was guided by structural insights from pharmacogenomic studies, which identified critical binding sites and mutations within the IL-6 protein. This approach ensured that our inhibitors specifically target these sites, enhancing their binding affinity and efficacy. Secondly, our compounds were designed to interact with both IL-6 protein and mRNA, providing a dual mechanism of action. This dual inhibition is significant because it addresses the IL-6 signaling pathway at multiple points, potentially leading to more effective and sustained therapeutic outcomes. Additionally, the favorable ADMET (Absorption, Distribution, Metabolism, Excretion, and Toxicity) profiles of our compounds further support their potential for effective IL-6 inhibition with minimal side effects.

Several interleukin-related drugs are currently in various stages of clinical trials, reflecting the ongoing efforts to target IL-6 and related cytokines for therapeutic purposes:

1. Tocilizumab: Targets both soluble and membrane-bound IL-6 receptors. It is approved for treating rheumatoid arthritis, Castleman disease, systemic juvenile idiopathic arthritis, giant cell arteritis, Takayasu arteritis, adult-onset Still's disease, cytokine storm in CAR T-cell therapy, and severe COVID-19 pneumonia. (Chugai, Roche, and Genentech) (Mihara et al. 2005).

2. Sarilumab: Aimed at IL-6 receptors, approved for COVID-19 and rheumatoid arthritis, and under investigation for lupus nephritis. (Sanofi and Regeneron) (Rafique et al. 2013).

3. Sirukumab: Targets IL-6 and is in clinical trials for COVID-19. (Janssen) (Mease et al. 2012).

4. Clazakizumab: Inhibits IL-6 and is being tested for chronic active antibody-mediated rejection in kidney transplants and organ transplant rejection. (Bristol Myers Squib and Alder) (Rafique et al. 2013).

5. Olokizumab: Targets IL-6 and is in trials for rheumatoid arthritis and Crohn's disease. (Conaris Research Institute, Ferring Pharmaceuticals, and I-Mab Biopharma) (Shaw et al. 2014).

6. Vobarilizumab: Aimed at IL-6 receptor, under investigation for rheumatoid arthritis and systemic lupus erythematosus. (Ablynx) (Garbers et al. 2018).

7. ALX-0061: Targets both soluble and membrane-bound IL-6 receptors and is in trials for rheumatoid arthritis (Van Roy et al. 2012).

These drugs represent a diverse range of approaches to targeting IL-6 and related interleukins, highlighting the significance of this pathway in treating inflammatory and autoimmune conditions.

Research into small molecules for IL-6 inhibition has revealed a range of compounds with varying mechanisms of action and effectiveness. LMT-28 demonstrated significant inhibition of IL-6-induced proliferation in TF-1 cells with an IC_{50} value of 7.5 μM, highlighting its potential in modulating IL-6 signaling (Park et al. 2021). Compounds featuring the 2,5-diaminobenzoxazole moiety, such as Compound 2a and Compound 2e, exhibited noteworthy inhibition of LPS-induced IL-6 production and IL-6 mRNA levels in RAW264.7 cells, showing their promise in inflammatory contexts (Yoo et al. 2022). SC-144, a quinoxalinhydrazide derivative, was effective in inhibiting cell growth in human ovarian cancer cell lines, demonstrating IC_{50} values in the low micromolar range. Raloxifene, traditionally used as a selective estrogen receptor modulator, has shown IL-6 inhibition in cancer cells, indicating its potential off-target effects (Hering et al. 2023). DB12903 and DB08402, developed through

pharmacophore modeling, exhibited high binding affinities with ΔGbind values of –118.30 and –267.09, respectively, underscoring their potential as potent IL-6 inhibitors (Tran et al. 2023). Further compounds such as Sch-24471 and SCH-21418 have been highlighted for their ability to decrease IL-6 levels in murine myelomonocytic leukemia cells by 90% and 87%, respectively (Tagat et al. 1995). Bazedoxifene, another selective estrogen receptor modulator, showed IL-6 inhibition in A-549 cells with an IC_{50} of 24.7 μM. Andrographolide and Micheliolide have demonstrated substantial inhibition of IL-6 production in RAW264.7 cells and gastric cancer cells, respectively. MDL-5 and MDL-16 exhibited potent inhibition of IL-6-induced cell proliferation in MCF-7 cells, with IC_{50} values of 5 μM and 20 μM, respectively (Aqel et al. 2019). Bergenin showed significant inhibition of IL-6-induced proliferation in THP-1 cells, with an IC_{50} value of 0.208 μM. 1-Benzyl-2,4,5-triphenyl-4,5-dihydro-1H-imidazole-derived compounds and benzophenone analogues demonstrated impressive inhibition of NF-κB-mediated IL-6 production and IL-6-induced proliferation in various cell lines, with IC_{50} values as low as 0.8 μM and high efficacy percentages (97% and 76% inhibition) (Sun et al. 2017; Salimo et al. 2023). Chalcone-based compounds showed inhibition of LPS-induced IL-6 production in RAW-264.7 cells with an IC50 of 5.55 nM, emphasizing their potency in targeting IL-6 (Wu et al. 2011). Collectively, these small molecules highlight the diverse approaches and effectiveness in targeting IL-6, though challenges remain in achieving specificity and optimizing their pharmacokinetic profiles for clinical use.

Our research brings a novel perspective to the development of IL-6 inhibitors by focusing on 1,3-indanedione derivatives. Unlike previous studies, we integrated bioisosterism to enhance the specificity and efficacy of our compounds. We performed a comprehensive pharmacogenomic analysis, identifying critical amino acid residues and mutations in the IL-6 protein that impact ligand binding. This guided the rational design of inhibitors tailored to these specific sites, improving their potential to disrupt IL-6 signaling. Our compounds, AKS7 and

AKS11, stand out due to their dual inhibitory activity against both IL-6 protein and mRNA expression. Their efficacy surpasses existing small molecules, supported by robust binding affinities and favorable pharmacokinetic profiles. This comprehensive approach not only advances our understanding of IL-6 inhibition but also sets a precedent for developing new therapeutic agents with significant clinical potential.

Our findings place our small molecules in a promising position compared to existing IL-6-targeted therapies, such as monoclonal antibodies and other small molecules. While monoclonal antibodies like Tocilizumab and Sarilumab have demonstrated clinical efficacy, they come with limitations including high cost and potential immunogenicity. In contrast, our small molecules offer a potentially more accessible and cost-effective alternative. The dual inhibitory activity of our compounds provides a unique advantage, addressing both IL-6 protein and mRNA levels. Future research will focus on optimizing these molecules further, assessing their effects in various disease models, and advancing them through clinical trials to establish their efficacy and safety. This work aims to complement existing IL-6 therapies and provide new solutions for managing chronic inflammatory and autoimmune diseases.

8. Conclusion

In conclusion, our comprehensive approach encompassing both in-silico and experimental studies has yielded promising results in the development of novel inhibitors targeting the IL-6 signaling pathway. Through in-silico screening, we identified lead compounds with favorable binding affinities to the IL-6 receptor, guiding our synthesis efforts. our study introduces the novel 1,3-indanedione analogues AKS7 and AKS11 as potent inhibitors of IL-6, a key cytokine implicated in various inflammatory conditions including rheumatoid arthritis. Through robust experimental validation, including RT-PCR and ELISA assays, we demonstrated the efficacy of AKS7 and AKS11 in inhibiting both IL-6 mRNA expression and protein production. Importantly, our compounds exhibited favorable safety profiles in acute oral toxicity studies,

highlighting their potential for clinical translation. Furthermore, in a rat model of arthritis, AKS7 and AKS11 significantly mitigated arthritis symptoms, underscoring their therapeutic potential in managing inflammatory diseases. The observed downregulation of key inflammatory genes IL-6 and STAT-3 further supports the candidacy of AKS7 and AKS11 for further development as IL-6 inhibitors in anti-arthritic therapies. Our synthesized compounds, particularly AKS7 and AKS11, demonstrate dual inhibitory actions on the IL-6 signaling pathway, effectively modulating IL-6-mediated inflammation through their actions on both IL-6 protein and mRNA expression, as well as STAT-3 gene expression. These findings underscore the therapeutic potential of our compounds for conditions associated with dysregulated IL-6/STAT-3 signaling pathways. Overall, our findings position AKS7 and AKS11 as promising candidates for advancing the treatment landscape of IL-6-mediated inflammatory disorders.

Abbreviations:

IL-6	: Interleukin-6
RA	: Rheumatoid Arthritis
SNP	: Single Nucleotide Polymorphism
TLRs	: Toll-Like Receptors
NF-κB	: Nuclear Factor Kappa B
TNF-α	: Tumor Necrosis Factor Alpha
JAK/STAT	: Janus Kinase/Signal Transducer and Activator of Transcription
DMEM	: Dulbecco's Modified Eagle Medium
FBS	: Fetal Bovine Serum
EDTA	: Ethylenediaminetetraacetic Acid
PCR	: Polymerase Chain Reaction

AKT	: Protein Kinase B
XP	: Extra Precision
ΔGbind	: Binding Free Energy Change
ΔGbind Coulomb	: Coulombic Interaction Energy Change
ΔGbind covalent	: Covalent Interaction Energy Change
ΔGbind Vander	: Van der Waals Interaction Energy Change
ΔGbind H-Bond	: Hydrogen Bonding Interaction Energy Change
ΔGbind Lipophilic	: Hydrophobic Interaction Energy Change
SAR	: Structure-Activity Relationship)

Declarations:

Ethics approval and consent to participate

Ethical approval (IAEC approval number: JSSCP/OT/IAEC/22/2022-2023) ensured adherence to humane treatment standards throughout the study.

Consent for publication

All the authors are consent for publication.

Availability of data and materials

Not applicable.

Competing interests

Not applicable.

Funding support

Not applicable.

Authors' contributions

All authors contributed equally.

Acknowledgment

Author Akey Krishna Swaroop expresses his gratitude to JSS College of Pharmacy, JSS Academy of Higher Education and Research.

References:

Akey KS, Jubie S, Vasanth P, et al (2021) Dual modulation of IL-6 pathway by flavonoid-metal complexes as immune boosters for SARS-CoV-2 therapy. SPAST Abstracts 1:

Aqel SI, Kraus EE, Jena N, et al (2019) Novel small molecule IL-6 inhibitor suppresses autoreactive Th17 development and promotes Treg development. Clinical & Experimental Immunology 196:215–225

Asadi S, Mohammadi Ziarani G (2016) The molecular diversity scope of 1, 3-indandione in organic synthesis. Molecular diversity 20:111–152

B. S. N, P. K. KN, Akey KS, et al (2023) Vitamin D analog calcitriol for breast cancer therapy; an integrated drug discovery approach. Journal of Biomolecular Structure and Dynamics 0:1–27. https://doi.org/10.1080/07391102.2023.2199866

Begam AJ, Basheer KA, Jubie S, et al (2019) A New Class of Pure Estrogen Alpha Receptor Antagonists; Design, Synthesis and in-vitro Screening. Letters in Drug Design & Discovery 16:66–81

Cai L, Zhan M, Li Q, et al (2020) DNA methyltransferase DNMT1 inhibits lipopolysaccharide-induced inflammatory response in human dental pulp cells involving the methylation changes of IL-6 and TRAF6. Molecular Medicine Reports 21:959–968. https://doi.org/10.3892/mmr.2019.10860

Chen G, Song Y, Ma F, Ma Y (2020) Anti-arthritic activity of D-carvone against complete Freund's adjuvant-induced arthritis in rats through modulation of inflammatory cytokines. Korean J Physiol Pharmacol 24:453–462

Chenicheri S, Ramachandran R, Rajamanikam U (2022) Antimicrobial effects of hydroxyapatite mosaicked polyvinyl alcohol-alginate semi-interpenetrating hydrogel-loaded with ethanolic extract of Glycyrrhiza glabra against oral pathogens. Prog Biomater 11:373–383. https://doi.org/10.1007/s40204-022-00199-2

Choy EH, De Benedetti F, Takeuchi T, et al (2020) Translating IL-6 biology into effective treatments. Nature Reviews Rheumatology 16:335–345

Cobleigh MA, Vogel CL, Tripathy D, et al (1999) Multinational study of the efficacy and safety of humanized anti-HER2 monoclonal antibody in women who have HER2-overexpressing metastatic breast cancer that has progressed after chemotherapy for metastatic disease. J Clin Oncol 17:2639–2648. https://doi.org/10.1200/JCO.1999.17.9.2639

Copaescu A, Smibert O, Gibson A, et al (2020) The role of IL-6 and other mediators in the cytokine storm associated with SARS-CoV-2 infection. Journal of Allergy and Clinical Immunology 146:518-534.e1. https://doi.org/10.1016/j.jaci.2020.07.001

D. G, PRAKASH M, RAMSESHU K (2007) Synthesis and Biological Evaluation of Substituted Thiophenyl Derivatives of Indane-1, 3-Dione. E-Journal of Chemistry 4:428–433. https://doi.org/10.1155/2007/865470

Dinarello CA (2007) Historical insights into cytokines. Eur J Immunol 37:S34–S45. https://doi.org/10.1002/eji.200737772

Elangovan A, Ramachandran J, Lakshmanan DK, et al (2022) Ethnomedical, phytochemical and pharmacological insights on an Indian medicinal plant: The balloon vine (*Cardiospermum halicacabum* Linn.). Journal of Ethnopharmacology 291:115143. https://doi.org/10.1016/j.jep.2022.115143

Feldmann M, Brennan FM (1996) Maini rn. Role of cytokines in rheumatoid arthritis Annu Rev Immunol 14:397–440

Frédérick R, Dumont W, Ooms F, et al (2006) Synthesis, structural reassignment, and biological activity of type B MAO inhibitors based on the 5 H-indeno [1, 2-c] pyridazin-5-one core. Journal of medicinal chemistry 49:3743–3747

Furman S, Nissim-Bardugo E, Zeeli S, et al (2014) Synthesis and in vitro evaluation of anti-inflammatory activity of ester and amine derivatives of indoline in RAW 264.7 and peritoneal macrophages. Bioorganic & Medicinal Chemistry Letters 24:2283–2287

Garbers C, Heink S, Korn T, Rose-John S (2018) Interleukin-6: designing specific therapeutics for a complex cytokine. Nature reviews Drug discovery 17:395–412

Garbers C, Hermanns HM, Schaper F, et al (2012) Plasticity and cross-talk of Interleukin 6-type cytokines. Cytokine & Growth Factor Reviews 23:85–97. https://doi.org/10.1016/j.cytogfr.2012.04.001

Genovese MC, Fleischmann R, Kivitz AJ, et al (2015) Sarilumab Plus Methotrexate in Patients With Active Rheumatoid Arthritis and Inadequate Response to Methotrexate: Results of a Phase III Study. Arthritis Rheumatol 67:1424–1437. https://doi.org/10.1002/art.39093

Heinrich PC, Behrmann I, Haan S, et al (2003) Principles of interleukin (IL)-6-type cytokine signalling and its regulation. Biochemical journal 374:1–20

Hering NA, Günzler E, Arndt M, et al (2023) Targeting Interleukin-6/Glycoprotein-130 Signaling by Raloxifene or SC144 Enhances Paclitaxel Efficacy in Pancreatic Cancer. Cancers 15:456

Hirose T, Sunazuka T, Shirahata T, et al (2002) Short total synthesis of (+)-madindolines A and B. Org Lett 4:501–503. https://doi.org/10.1021/ol017058i

Hong S-S, Choi JH, Lee SY, et al (2015) A novel small-molecule inhibitor targeting the IL-6 receptor β subunit, glycoprotein 130. The Journal of Immunology 195:237–245

Hunter CA, Jones SA (2015) IL-6 as a keystone cytokine in health and disease. Nature immunology 16:448–457

Ingawale DK, Patel SS (2018) Hecogenin exhibits anti-arthritic activity in rats through suppression of pro-inflammatory cytokines in Complete Freund's adjuvant-induced arthritis. Immunopharmacology and Immunotoxicology 40:59–71. https://doi.org/10.1080/08923973.2017.1405439

Jones GW, McLoughlin RM, Hammond VJ, et al (2010) Loss of CD4+ T cell IL-6R expression during inflammation underlines a role for IL-6 trans signaling in the local maintenance of Th17 cells. The journal of immunology 184:2130–2139

Jones SA, Jenkins BJ (2018) Recent insights into targeting the IL-6 cytokine family in inflammatory diseases and cancer. Nature reviews immunology 18:773–789

Kamel KM, Gad AM, Mansour SM, et al (2018) Novel Anti-arthritic Mechanisms of Polydatin in Complete Freund's Adjuvant-Induced Arthritis in Rats: Involvement of IL-6, STAT-3, IL-17, and NF-κB. Inflammation 41:1974–1986. https://doi.org/10.1007/s10753-018-0841-4

Kang S, Tanaka T, Kishimoto T (2015) Therapeutic uses of anti-interleukin-6 receptor antibody. International immunology 27:21–29

Kaur S, Bansal Y, Kumar R, Bansal G (2020) A panoramic review of IL-6: Structure, pathophysiological roles and inhibitors. Bioorganic & medicinal chemistry 28:115327

Kishimoto T, Kang S (2022) IL-6 Revisited: From Rheumatoid Arthritis to CAR T Cell Therapy and COVID-19. Annu Rev Immunol 40:323–348. https://doi.org/10.1146/annurev-immunol-101220-023458

Krishna Swaroop A, Krishnan Namboori PK, Esakkimuthukumar M, et al (2023) Leveraging decagonal in-silico strategies for uncovering IL-6 inhibitors with precision. Computers in Biology and Medicine 163:107231. https://doi.org/10.1016/j.compbiomed.2023.107231

Krishna Swaroop A, Kumar Patnaik S, P V, et al (2022) Design and synthesis of novel quercetin metal complexes as IL-6 inhibitors for anti-inflammatory effect in SARS-CoV-2. Indian Journal of Biochemistry and Biophysics (IJBB) 59:824–836. https://doi.org/10.56042/ijbb.v59i8.55954

Lesina M, Kurkowski MU, Ludes K, et al (2011) Stat3/Socs3 activation by IL-6 transsignaling promotes progression of pancreatic intraepithelial neoplasia and development of pancreatic cancer. Cancer cell 19:456–469

Li C, Fuchs J, Lin J, COLUMBUS OSU (2013) Novel Small Molecules Disabling the IL-6/IL-6R/GP130 Heterohexamer Complex

M E, Krishna Swaroop A, Kumar Patnaik S, et al (2022) A novel family of small molecule HIF-1 alpha stabilizers for the treatment of diabetic wounds; an integrated in silico , in vitro , and in vivo strategy. RSC Advances 12:31293–31302. https://doi.org/10.1039/D2RA05364K

Mauer J, Chaurasia B, Goldau J, et al (2014) Signaling by IL-6 promotes alternative activation of macrophages to limit endotoxemia and obesity-associated resistance to insulin. Nature immunology 15:423–430

May U, Schiffelholz T, Baier PC, et al (2009) IL-6-trans-signalling increases rapid-eye-movement sleep in rats. European journal of pharmacology 613:141–145

Mease P, Strand V, Shalamberidze L, et al (2012) A phase II, double-blind, randomised, placebo-controlled study of BMS945429 (ALD518) in patients with rheumatoid arthritis with an inadequate response to methotrexate. Annals of the rheumatic diseases 71:1183–1189

Meena S, Shankar D, Ramseshu KV, et al (2006) Synthesis of 2-(Arylmethylene)-(1H)-indane-1,3-(2H)-diones as Potential Fungicidal and Bactericidal Agents. ChemInform 37:. https://doi.org/10.1002/chin.200640094

Mihara M, Kasutani K, Okazaki M, et al (2005) Tocilizumab inhibits signal transduction mediated by both mIL-6R and sIL-6R, but not by the receptors of other members of IL-6 cytokine family. International Immunopharmacology 5:1731–1740. https://doi.org/10.1016/j.intimp.2005.05.010

Mitka K, Kowalski P, Pawelec D, Majka Z (2009) Synthesis of Novel Indane-1,3-dione Derivatives and Their Biological Evaluation as Anticoagulant Agents. Croatica Chemica Acta 82:613

Mude L, Jupudi S, Swaroop AK, et al (2023) Molecular insights in repurposing selective COX-2 inhibitor celecoxib against matrix metalloproteinases in potentiating delayed wound healing: a molecular docking and MMPB/SA based analysis of molecular dynamic simulations. Journal of Biomolecular Structure and Dynamics 1–12. https://doi.org/10.1080/07391102.2023.2209666

Namboori PK (2021) Identification of lapatinib derivatives and analogs to control metastatic breast cancer-specific to South Asian population-a pharmacogenomic approach. WSEAS Transactions on Biology and Biomedicine 18:51–62

Narazaki M, Kishimoto T (2022) Current status and prospects of IL-6–targeting therapy. Expert Review of Clinical Pharmacology 15:575–592. https://doi.org/10.1080/17512433.2022.2097905

Nyati KK, Kishimoto T (2022) Recent Advances in the Role of Arid5a in Immune Diseases and Cancer. Front Immunol 12:. https://doi.org/10.3389/fimmu.2021.827611

Nyati KK, Kishimoto T (2023) The emerging role of Arid5a in cancer: A new target for tumors. Genes & Diseases 10:813–824. https://doi.org/10.1016/j.gendis.2021.12.012

Park Y-H, Jang Y-J, Choi Y, et al (2021) Combination of LMT-28 and metformin improves beneficial anti-inflammatory effect in collagen-induced arthritis. Pharmacology 106:53–59

Patnaik SK, Ayyamperumal S, Jade D, et al (2024) Virtual high throughput screening of natural peptides against ErbB1 and ErbB2 to identify potential inhibitors for cancer chemotherapy. Journal of Biomolecular Structure and Dynamics 42:5551–5574. https://doi.org/10.1080/07391102.2023.2226744

Peng Y, Yang Q, Gao S, et al (2022) IL-6 protects cardiomyocytes from oxidative stress at the early stage of LPS-induced sepsis. Biochemical and Biophysical Research Communications 603:144–152. https://doi.org/10.1016/j.bbrc.2022.03.013

Pluskota R, Koba M (2018) Indandione and Its Derivatives - Chemical Compounds with High Biological Potential. Mini Rev Med Chem 18:1321–1330. https://doi.org/10.2174/1389557518666180330101809

Rafique A, Martin J, Blome M, et al (2013) AB0037 Evaluation of the binding kinetics and functional bioassay activity of sarilumab and tocilizumab to the human il-6 receptor (il-6r) alpha. Annals of the Rheumatic Diseases 72:A797–A797

Rose-John S (2018) Interleukin-6 family cytokines. Cold Spring Harbor perspectives in biology 10:a028415

S. M, S. J, C. P, et al Synthesis and screening of cyclic diketone indanedione derivatives as future scaffolds for neutrophil elastase inhibition. RSC Adv 13:11838–11852. https://doi.org/10.1039/d3ra00106g

Salama C, Han J, Yau L, et al (2021) Tocilizumab in Patients Hospitalized with Covid-19 Pneumonia. N Engl J Med 384:20–30. https://doi.org/10.1056/NEJMoa2030340

Salimo ZM, Yakubu MN, da Silva EL, et al (2023) Chemistry and pharmacology of bergenin or its derivatives: A promising molecule. Biomolecules 13:403

Schaper F, Rose-John S (2015) Interleukin-6: Biology, signaling and strategies of blockade. Cytokine & growth factor reviews 26:475–487

Selvaraj NB, Swaroop AK, Mariappan E, et al (2023) Effect of Calcitriol in Inhibiting the Cancer Cell Growth and Promoting Apoptosis in ErbB2-positive Breast Cancer Cells. Anticancer Agents Med Chem 23:2056–2071. https://doi.org/10.2174/1871520623666230822100006

Shaw S, Bourne T, Meier C, et al (2014) Discovery and characterization of olokizumab: A humanized antibody targeting interleukin-6 and neutralizing gp130-signaling. mAbs 6:773–781. https://doi.org/10.4161/mabs.28612

Singh K (2016) Applications of indan-1, 3-dione in heterocyclic synthesis. Current Organic Synthesis 13:385–407

Skiniotis G, Boulanger MJ, Garcia KC, Walz T (2005) Signaling conformations of the tall cytokine receptor gp130 when in complex with IL-6 and IL-6 receptor. Nature structural & molecular biology 12:545–551

Sommer J, Engelowski E, Baran P, et al (2014) Interleukin-6, but not the interleukin-6 receptor plays a role in recovery from dextran sodium sulfate-induced colitis. International journal of molecular medicine 34:651–660

Sun Z, Li G, Tong T, Chen J (2017) Micheliolide suppresses LPS-induced neuroinflammatory responses. PLoS One 12:e0186592

Swaroop AK, Lalitha CMVN, Shanmugam M, et al (2022a) Plant Derived Immunomodulators; A Critical Review. Adv Pharm Bull 12:712–729. https://doi.org/10.34172/apb.2022.074

Swaroop AK, Nagarjuna P, Naresh P, et al (2022b) Discovery of Immunomodulators from Plant Kingdom Targeting IL-6 for the Effective Management Therapy of SARS-CoV-2. Journal of Natural Remedies 249–260

Swaroop AK, Negi P, Kar A, et al (2024) Navigating IL-6: From molecular mechanisms to therapeutic breakthroughs. Cytokine Growth Factor Rev 76:48–76. https://doi.org/10.1016/j.cytogfr.2023.12.007

Tagat JR, Nazareno DV, McCombie SW, et al (1995) Synthetic inhibitors of interleukin-6 I: 2,3,7,8-tetrahydro-4-aryl-1H-cyclopent [e] imidazo [1,2-a]- pyridin-5(6H)-one and related compounds. Bioorganic & Medicinal Chemistry Letters 5:2139–2142. https://doi.org/10.1016/0960-894X(95)00362-W

Tanaka T, Kishimoto T (2014) The biology and medical implications of interleukin-6. Cancer immunology research 2:288–294

Tanaka T, Narazaki M, Kishimoto T (2012) Therapeutic Targeting of the Interleukin-6 Receptor. Annu Rev Pharmacol Toxicol 52:199–219. https://doi.org/10.1146/annurev-pharmtox-010611-134715

Tran Q-H, Nguyen Q-T, Tran T-TN, et al (2023) Identification of small molecules as potential inhibitors of interleukin 6: a multi-computational investigation. Mol Divers 27:2315–2330. https://doi.org/10.1007/s11030-022-10558-7

Van Roy M, Van de Sompel A, De Smet K, et al (2012) ALX-0061, an Anti-IL-6R Nanobody® forUse in Rheumatoid Arthritis, Demonstrates a Different In Vitro Profile as Compared to Tocilizumab. International journal of biological sciences 8:1237–47

Verma G, Marella A, Shaquiquzzaman M, et al (2014) A review exploring biological activities of hydrazones. J Pharm Bioallied Sci 6:69–80. https://doi.org/10.4103/0975-7406.129170

Wang Y, Du P, Jiang D (2020) Berberine functions as a negative regulator in lipopolysaccharide - induced sepsis by suppressing NF-κB and IL-6 mediated STAT3 activation. Pathogens and Disease 78:ftaa047. https://doi.org/10.1093/femspd/ftaa047

Wu J, Li J, Cai Y, et al (2011) Evaluation and Discovery of Novel Synthetic Chalcone Derivatives as Anti-Inflammatory Agents. J Med Chem 54:8110–8123. https://doi.org/10.1021/jm200946h

Yoo J, Kim D, Park J, et al (2022) Novel small molecule inhibitors targeting the IL-6/STAT3 pathway or IL-1β. Molecules 27:2696